

# A Measure of Predictive Sharpness for Probabilistic Models

Pekka Syrjänen\*  
 University of Helsinki

## Abstract

This paper introduces a measure of predictive sharpness for probabilistic models, capturing the extent to which predictive mass departs from uniformity and concentrates over narrower subsets of the domain. For discrete settings, the measure is defined by cumulatively quantifying deviation from uniformity, taking into account both exclusion of outcomes and concentration of probability mass. For continuous settings, we develop an integral representation based on a monotone rearrangement of the predictive density. In supplementary material, we establish mathematical properties of the measure, derive formulas for forward and inverse domain transformations to support cross-domain comparisons, and provide an analysis of the relationship of the measure with entropy and variance.

*Keywords:* *Predictive sharpness; Predictive distribution; Probabilistic forecast*

## 1 Introduction

Probabilistic forecasts play an increasingly central role in statistical modeling, scientific inference, and applied decision-making. Beyond accuracy and calibration, one of the key desiderata of probabilistic prediction is sharpness—the concentration of the predictive distribution (Gneiting et al. 2007, Gneiting & Raftery 2007, Gneiting & Katzfuss 2014). Sharpness is a property of the forecast only (Gneiting & Katzfuss 2014). Yet, sharpness is critical for interpretability, actionability, and scientific informativeness: a forecast that distributes mass diffusely, even if calibrated, conveys limited practical information.

---

\*pekka.syrjanen@helsinki.fi

Despite its importance, no measure currently exists that quantifies predictive sharpness consistently across both discrete and continuous domains. Sharpness is typically assessed alongside calibration as a component of proper scoring rules such as the continuous ranked probability score (CRPS) (Gneiting & Raftery 2007). When reported separately, prediction interval width is a commonly used metric (Gneiting & Katzfuss 2014). However, these methods have limitations. For example, while measures such as CRPS decompose empirically to discrimination, uncertainty, and miscalibration components (Arnold et al. 2024), a distinct and interpretable measure of sharpness—applicable both pre-observationally and to single probabilistic predictions—has not been provided. Furthermore, although CRPS is used widely in aggregate evaluations, it is less discerning in individual cases and may yield favorable scores even when the realized outcome lies outside high-density regions of the predictive distribution (Du 2021). Prediction interval width, while indicating where the model is most confident, provides only a coarse view of the concentration within the distribution.

In this paper, we introduce a new measure of predictive sharpness that addresses these gaps. The proposed sharpness measure is defined for both discrete and continuous probability distributions and is designed to quantify how strongly a prediction concentrates mass over regions of a domain. As a key feature of interpretability, the measure is bounded within the unit interval  $[0,1]$ , where 0 corresponds to a uniform distribution (maximal vagueness) and 1 corresponds to a degenerate distribution (point prediction of a single outcome). Proofs of key mathematical properties are provided in the supplementary material.

For discrete settings, the measure is defined by cumulatively quantifying deviation from uniformity, taking into account both exclusion of outcomes and the concentration of probability mass. The continuous version of the measure is constructed using a monotone rearrangement of the predictive density. This yields a novel, geometrically grounded

formulation in which sharpness is expressed as a mass–length integral over a functional representation of the outcome space. The mass-length formulation provides a structured space in which aspects of the original distribution can be analyzed alongside sharpness, also enabling a detailed decomposition of the sharpness score. Additionally, we establish a mathematical link to the classical Gini coefficient, connecting the measure to robust statistical applications. For both discrete and continuous cases, a simplified expression is derived for computational efficiency. Additional technical results are presented in the supplementary material, including derivations of forward and inverse domain transformations for cross-domain comparison and an extended analysis of the relationships between sharpness, entropy, and variance.

From a practical standpoint, the proposed measure is easy to compute and applicable across a broad range of probabilistic modeling contexts. In contrast to two widely used information-theoretic criteria—Shannon entropy and Kullback–Leibler (KL) divergence—the sharpness measure is normalized and responds predictably and proportionally to changes in the concentration of probability mass. Numerical examples in Section 3 highlight how the measure responds to changes in distributional shape and concentration, and how it complements standard information-theoretic criteria by offering a focused lens on probabilistic concentration.

In practical applications, the measure enables disentangling sharpness from accuracy and calibration for a broad range of models. The measure complements traditional scoring rules such as CRPS, providing accompanying information about the sharpness of the distribution for both ensemble forecasts and single probabilistic predictions. Importantly, however, the sharpness measure does not constitute a scoring rule and its chief applications lie in model diagnostics, where it is best used in conjunction with other diagnostic measures, including variance, calibration, and further information-theoretic criteria. Its primary role is to isolate

and quantify predictive concentration. Further potential applications include Bayesian analysis, model selection, and hypothesis evaluation.

The structure of the paper is as follows. In Section 2, we derive the measure of predictive sharpness, beginning with discrete deterministic cases and extending it to discrete and continuous probabilistic domains. We further observe the generalizability of the measure to multidimensional cases, and define a relative measure of predictive sharpness. Section 3 presents numerical examples with comparisons to Shannon entropy, Kullback–Leibler divergence, and variance. Section 4 discusses the geometric properties of the measure, including a Gini-type formulation. Section 5 presents applications, focusing on the applicability of the measure as a model diagnostic tool. Section 6 discusses limitations and extensions.

## 2 A Measure of Predictive Sharpness

We introduce a measure of predictive sharpness, motivated by the goal of quantifying the extent to which a probabilistic prediction concentrates mass over subsets or regions of an outcome space.

### 2.1 Sharpness in Discrete Outcome Spaces

Consider the case in which the outcome space  $\gamma = \text{Dom}(f)$  is finite, comprising  $n = |\gamma|$  mutually exclusive and exhaustive elements, and the predictions are given deterministically. In a deterministic setting, a natural candidate for measuring concentration over subsets of the outcome space is the fraction of ruled-out outcomes, relative to the maximum number of outcomes that can be excluded,  $n - 1$ . Let  $r$  denote the number of outcomes excluded by a prediction. We define a deterministic measure of predictive sharpness by

$$S_{\text{DET}} = \frac{r}{n - 1}, \quad (2.1)$$

so that  $S_{\text{DET}} = 0$  when no outcomes are ruled out and  $S_{\text{DET}} = 1$  when all but one outcome are excluded. Thus, for example, with  $n = 4$ , exclusion of any one outcome yields  $S_{\text{DET}} = 1/3$  and the exclusion of any two yields  $S_{\text{DET}} = 2/3$ .

This deterministic notion of predictive sharpness can be extended to probabilistic predictions over  $\gamma = \{y_1, \dots, y_n\}$ , where uncertainty over the outcomes is expressed by a probability mass function  $P = \{p_1, \dots, p_n\}$ . In the probabilistic setting, a maximally diffuse prediction corresponds to the uniform distribution over  $\gamma$ , reflecting total uncertainty over the domain. Predictive concentration increases as the distribution diverges from uniformity by concentrating mass over narrower subsets of the outcomes.

In first approximation, we consider the total variation distance (TVD) from the uniform, which we can further normalize to the unit interval for alignment with  $S_{\text{DET}}$ . This yields:

$$\text{TVD}_S = \frac{\sum_{i=1}^n |p_i - 1/n|}{2(1 - 1/n)}, \quad (2.2)$$

where  $p_i$  is the probability of  $y_i$  in  $\gamma = \{y_1, \dots, y_n\}$ . However, this measure fails to distinguish between distributions that differ in the concentration of mass within the support of the distribution. For example, when  $|\gamma| = 4$ ,  $\text{TVD}_S$  yields the same score of  $2/3$  for distributions such as  $\{0, 0, 0.5, 0.5\}$  and  $\{0, 0, 0.25, 0.75\}$ , despite the latter reflecting a sharper prediction over the outcome space. Thus,  $\text{TVD}_S$  misses many local shifts in the concentration of probability mass within the distribution, highlighting the need for a more refined measure sensitive to both exclusion and concentration.

To construct a more refined measure of probabilistic concentration, we begin by examining how the probability of particular outcomes deviates from the uniform baseline as a prediction concentrates over a subset of the outcomes. Assigning zero probability to an outcome represents maximal exclusion and should thus correspond to the value of exclusion given by  $S_{\text{DET}}$ . By contrast, a partial reduction relative to the uniform should contribute proportionally less. For instance, in a four-element outcome space, fully eliminating one

outcome should contribute  $1/3$  to the probabilistic sharpness score, while reducing the probability of an outcome by  $1/2$  relative to the uniform should correspond to a lesser, proportional contribution, here  $1/6$ .

To ensure consistency between the outcomes, however, we observe that the measure must remain context-sensitive: specifically, it must take into account the distribution of probability mass over the remaining, non-excluded outcomes. Consider again the four-element outcome space, where two outcomes are fully excluded. In the deterministic case,  $S_{\text{DET}}$  yields  $2/3$ , reflecting the exclusion of two outcomes. However, in the probabilistic case, this implies that the remaining two outcomes must each carry probability  $1/2$ . If, instead, the remaining mass is unequally distributed—for example,  $1/4$  and  $3/4$ —the distribution reflects greater concentration, and the value of the sharpness measure must accordingly exceed  $2/3$ . Hence, a suitable measure that reflects predictive sharpness in discrete probabilistic cases must track both global exclusion and concentration and local concentration over the remaining outcomes, maintaining comparability between the outcomes.

This motivates a construction in which concentration is quantified in a stepwise, cumulative manner. As probability mass concentrates, the relevant comparison set—the effective outcome space—shrinks. Sharpness, then, is quantified by assessing at each step how much the assigned mass undercuts the uniform distribution over the remaining outcomes, with each contribution computed relative to the remaining mass. Proceeding in order of increasing probability values, we assess the local contribution to the sharpness score by comparing the probability of each outcome to the corresponding local uniform and the remaining mass, where the latter reflects the global concentration within the distribution. After  $n - 1$  such steps, the final remaining outcome (the most probable one) carries the residual mass, with the entire distribution accounted for.

Let  $\{p_{(j)}\}_{j=1}^n$  be the predicted probabilities sorted in ascending order, so that  $p_{(1)} \leq p_{(2)} \leq$

$\dots \leq p_{(n)}$ . We then define  $m_{(j)} = \sum_{k=j}^n p_{(k)}$ , the total remaining probability mass at step  $j$ , and  $L_{(j)} = n - j + 1$ , the number of remaining outcomes at step  $j$ . Under local uniformity,  $p_{(j)} = m_{(j)}/L_{(j)}$ . At each step  $j$ , the local deviation from uniformity is thus the relative shortfall of the current probability from this uniform benchmark:

$$\left(1 - \frac{p_{(j)}}{m_{(j)}/L_{(j)}}\right).$$

Multiplying by the remaining mass yields

$$m_{(j)} - p_{(j)}L_{(j)},$$

which reflects, proportionally, the share of probability mass displaced upward to higher probability outcomes as the predicted probability undercuts its local uniform share. Summing up the local shortfalls and normalizing by the number of steps yields the proposed sharpness measure:

$$S(P) = \frac{1}{n-1} \sum_{j=1}^{n-1} (m_{(j)} - p_{(j)}L_{(j)}). \quad (2.3)$$

This expression quantifies the extent to which the predicted distribution diverges from uniformity in favor of more concentrated predictions. When  $P$  is uniform,  $S(P) = 0$ . When all but one outcome are fully excluded (i.e., assigned zero probability),  $S(P) = 1$ . In intermediate cases, the measure picks up any shift in probability mass towards increased concentration, rewarding this with increased sharpness score.

This expression obtains equal weight for each outcome with equal probability. However, we observe that the formula can also be rewritten in a more computationally efficient form (albeit losing decomposability). Collecting the coefficients on each  $p_{(j)}$ , the total coefficient on  $p_{(j)}$  is simply:

$$\frac{1}{n-1} (j - (n - j + 1)) = \frac{2j - n - 1}{n-1}.$$

This yields an equivalent, more compact expression:

$$S(P) = \sum_{j=1}^n \left( \frac{2j - n - 1}{n-1} \right) p_{(j)}. \quad (2.4)$$

$S(P)$  is applied in Section 3.1 to numerical examples and compared to Shannon entropy, Kullback–Leibler divergence, and variance.

## 2.2 Sharpness in Continuous Outcome Spaces

$S(P)$  extends naturally to continuous probabilistic settings, using the same cumulative approach. In the continuous setting, concentration is computed relative to the size of the domain.

Let  $\Omega \subset \mathbb{R}$  be a bounded, measurable domain with finite Lebesgue measure  $|\Omega| < \infty$ , and let  $d: \Omega \rightarrow \mathbb{R}_{\geq 0}$  be a probability density function over  $\Omega$  such that  $\int_{\Omega} d(y) dy = 1$ . To generalize the sharpness measure to continuous cases, we make use of the non-decreasing rearrangement of the probability density function, denoted  $d_*(t)$ , defined over the interval  $[0, |\Omega|]$ . This function reorders the values of  $d$  in increasing order with respect to Lebesgue measure. Formally,  $d_*(t)$  is defined such that:

$$d_*(t) = \inf \{s \geq 0 \mid \lambda(\{y \in \Omega \mid d(y) \leq s\}) \geq t\}.$$

This ordering reflects the ordering of the probability values with  $S(P)$ . We define  $m(t) = \int_t^{|\Omega|} d_*(s) ds$ , the remaining probability mass at  $t$ , and  $L(t) = |\Omega| - t$ , the remaining length of the domain at  $t$ . The continuous sharpness measure is then given by

$$S(d_*) = \frac{1}{|\Omega|} \int_0^{|\Omega|} (m(t) - d_*(t)L(t)) dt. \quad (2.5)$$

This expression quantifies how much the distribution deviates from uniformity, tracking the concentration of probability mass over regions of the domain. This measure satisfies the following properties:

- (a)  $S(d_*) = 0$  if  $d(y) = 1/|\Omega|$  for all  $y \in \Omega$ .
- (b)  $S(d_*) \rightarrow 1$  as  $d$  converges to a Dirac measure (i.e., exact point prediction).

(c) If the prediction is an interval  $[a, b] \subset \Omega$  with uniform density over  $[a, b]$ , then  $S(d_*) = 1 - \frac{b-a}{|\Omega|}$ .

Proof of normalization is provided in the supplementary material. We proceed to show (c) next:

**Proposition 2.1.** *Let  $\Omega \subset \mathbb{R}$  be a bounded measurable domain with finite Lebesgue measure  $|\Omega| < \infty$ . Suppose  $d: \Omega \rightarrow \mathbb{R}_{\geq 0}$  is a probability density function of the form*

$$d(y) = \frac{1}{\ell} \cdot \mathbf{1}_A(y),$$

where  $A \subset \Omega$  is a measurable subset of length  $\ell = |A|$ . Then the continuous sharpness measure satisfies

$$S(d_*) = 1 - \frac{\ell}{|\Omega|},$$

if  $A$  is a single interval or a union of disjoint intervals.

*Proof.* Since  $d(y) = \frac{1}{\ell}$  on a measurable subset  $A \subset \Omega$  with  $|A| = \ell$  and zero elsewhere, the non-decreasing rearrangement  $d_*(t)$  over  $[0, |\Omega|]$  is given by

$$d_*(t) = \begin{cases} 0, & 0 \leq t < |\Omega| - \ell, \\ \frac{1}{\ell}, & |\Omega| - \ell \leq t \leq |\Omega|, \end{cases}$$

We now evaluate the sharpness measure:

$$S(d_*) = \frac{1}{|\Omega|} \left( \int_0^{|\Omega|} m(t) dt - \int_0^{|\Omega|} d_*(t) L(t) dt \right),$$

where  $m(t) = \int_t^{|\Omega|} d_*(s) ds$  and  $L(t) = |\Omega| - t$ .

First, we compute  $\int_0^{|\Omega|} m(t) dt$ .

For  $0 \leq t < |\Omega| - \ell$ , we have

$$m(t) = \int_t^{|\Omega|-\ell} 0 ds + \int_{|\Omega|-\ell}^{|\Omega|} \frac{1}{\ell} ds = 1.$$

For  $|\Omega| - \ell \leq t \leq |\Omega|$ , we have

$$m(t) = \int_t^{|\Omega|} \frac{1}{\ell} ds = \frac{|\Omega| - t}{\ell}.$$

Thus,

$$\int_0^{|\Omega|} m(t) dt = \int_0^{|\Omega| - \ell} 1 dt + \int_{|\Omega| - \ell}^{|\Omega|} \frac{|\Omega| - t}{\ell} dt = |\Omega| - \ell + \frac{1}{\ell} \cdot \frac{\ell^2}{2} = |\Omega| - \frac{\ell}{2}.$$

We then evaluate  $\int_0^{|\Omega|} d_*(t) L(t) dt$ .

Since  $d_*(t) = 0$  on  $[0, |\Omega| - \ell]$ , we have

$$\int_0^{|\Omega|} d_*(t) L(t) dt = \int_{|\Omega| - \ell}^{|\Omega|} \frac{1}{\ell} (|\Omega| - t) dt = \frac{1}{\ell} \cdot \frac{\ell^2}{2} = \frac{\ell}{2}.$$

Combining:

$$S(d_*) = \frac{1}{|\Omega|} \left( |\Omega| - \frac{\ell}{2} - \frac{\ell}{2} \right) = \frac{1}{|\Omega|} (|\Omega| - \ell) = 1 - \frac{\ell}{|\Omega|}.$$

□

Similarly to  $S(P)$ ,  $S(d_*)$  simplifies to a more computationally efficient expression. Using Fubini's theorem:

$$\int_0^{|\Omega|} m(t) dt = \int_0^{|\Omega|} \left( \int_t^{|\Omega|} d_*(s) ds \right) dt = \int_0^{|\Omega|} d_*(s) \left( \int_0^s dt \right) ds = \int_0^{|\Omega|} s d_*(s) ds.$$

Next, rewrite the second term:

$$\begin{aligned} \int_0^{|\Omega|} d_*(t) L(t) dt &= \int_0^{|\Omega|} d_*(t) (|\Omega| - t) dt \\ &= |\Omega| \int_0^{|\Omega|} d_*(t) dt - \int_0^{|\Omega|} t d_*(t) dt \\ &= |\Omega| - \int_0^{|\Omega|} t d_*(t) dt. \end{aligned}$$

Substituting both into the definition:

$$\begin{aligned} S(d_*) &= \frac{1}{|\Omega|} \left( \int_0^{|\Omega|} s d_*(s) ds - \left( |\Omega| - \int_0^{|\Omega|} t d_*(t) dt \right) \right) \\ &= \frac{1}{|\Omega|} \left( \int_0^{|\Omega|} t d_*(t) dt + \int_0^{|\Omega|} t d_*(t) dt - |\Omega| \right) \end{aligned}$$

$$= \frac{2}{|\Omega|} \int_0^{|\Omega|} t d_*(t) dt - 1. \quad (2.6)$$

$S(d_*)$  provides a continuous analogue of the discrete sharpness measure, where it reflects the concentration of mass over subsets of the outcome space. The behavior of the measure is demonstrated in Section 3.2 through numerical examples, with comparisons to Shannon entropy and Kullback–Leibler divergence.

### 2.3 Relative Sharpness

$S(P)$  and  $S(d_*)$  are defined relative to the uniform baseline over the domain. In applied contexts, different baselines exist reflecting current benchmarks. Thus, it is useful to quantify also the relative increase in sharpness achieved by one distribution over another.

Let  $S_1, S_2 \in [0, 1]$  denote the sharpness scores of two predictive distributions defined over the same outcome space, with  $S_2 > S_1$ . We define the relative sharpness gain as:

$$\Delta S_{\text{REL}} := \frac{S_2 - S_1}{1 - S_1}. \quad (2.7)$$

This measure satisfies the following properties:

- (a)  $\Delta S_{\text{REL}} = 0$  if and only if  $S_1 = S_2$ ,
- (b)  $\Delta S_{\text{REL}} = 1$  if and only if  $S_2 = 1$ ,
- (c)  $\Delta S_{\text{REL}} \in (0, 1)$  where  $S_1 < S_2 < 1$ .

As the measure is normalized relative to the available margin for improvement, it facilitates comparisons across contexts with differing baselines. For example, consider a scenario in which an initial prediction yields  $S(d_*) = 0.98$ , and a refined prediction yields  $S(d_*) = 0.999$ . Then, the relative sharpness gain is:

$$\Delta S_{\text{REL}} = \frac{0.999 - 0.98}{1 - 0.98} = 0.95,$$

indicating that the refined prediction achieved 95 % of the possible increase in the sharpness score over this baseline (with the maximum value 1.0 corresponding to a deterministic prediction over the domain).

## 2.4 Extension to Multidimensional Domains

The sharpness measures  $S(P)$  and  $S(d_*)$  extend naturally also to multidimensional outcome spaces. Let  $\Omega \subset \mathbb{R}^d$ , for  $d \geq 1$ , be a bounded, Lebesgue-measurable domain with finite volume  $|\Omega| < \infty$ , and let  $d: \Omega \rightarrow \mathbb{R}_{\geq 0}$  be a probability density function satisfying  $\int_{\Omega} d(y) dy = 1$ . In the case of  $S(d_*)$ , we define the multidimensional measure of sharpness by applying the same rearrangement-based procedure used in the one-dimensional case. Specifically, we construct the non-decreasing rearrangement  $d_*: [0, |\Omega|] \rightarrow \mathbb{R}_{\geq 0}$ , defined over a one-dimensional interval of measure  $|\Omega|$ , such that for all  $t \in [0, |\Omega|]$ ,

$$d_*(t) = \inf \{s \geq 0 \mid \lambda(\{y \in \Omega \mid d(y) \leq s\}) \geq t\},$$

where  $\lambda$  denotes the Lebesgue measure. This rearrangement is defined by sorting the values of  $d(y)$  in increasing order with respect to Lebesgue measure, regardless of the underlying dimensions of  $\Omega$ . The sharpness score is then computed via the same formula used in the one-dimensional case (Equations 2.5 and 2.6). As in the one-dimensional case, the rearrangement  $d_*$  reflects the suppression of low-density regions in favor of more concentrated ones. The extension relies only on the existence of a total ordering of the density values, not on any particular coordinate structure. Hence, the measure is also defined for finite multidimensional domains equipped with a Lebesgue measure.

## 3 Numerical Examples

The predictive sharpness measure introduced above provides a way to quantify how strongly a probabilistic prediction concentrates mass over subsets of an outcome space. In this section,

we illustrate the behavior of the measure through numerical examples, with comparisons to Shannon entropy and Kullback–Leibler (KL) divergence. We further observe a reciprocal relationship with variance, where sharpness quantifies concentration as variance quantifies dispersion.

### 3.1 Discrete Distributions

We begin with the discrete case, examining a case where the outcome space consists of  $n = 4$  mutually exclusive and exhaustive outcomes. Table 1 reports the values of the sharpness measure  $S(P)$ , Shannon entropy (in bits), KL-divergence from the uniform distribution (also in bits), and variance for illustrative distributions.  $S(P)$  aligns with entropy and the corresponding divergence in rank order, but moves less sharply when approaching maximum concentration over the space of possibilities (i.e., only one outcome remains). At each step,  $S(P)$  reflects proportionally the degree of concentration over the outcome space.

Table 1: Sharpness scores for discrete probability distributions over  $|\gamma| = 4$ . Entropy and KL-divergence are expressed in bits. For variance calculation, the categories are defined as numerical (0,1,2,3).

<b>Distribution</b>	<b>S(P)</b>	<b>Shannon Entropy</b>	<b>KL-Divergence</b>	<b>Variance</b>
{0.25, 0.25, 0.25, 0.25}	0.000	2.000	0.000	1.250
{0.24, 0.24, 0.28, 0.24}	0.040	1.997	0.003	1.2096
{0, 1/3, 1/3, 1/3}	0.333	1.585	0.415	0.667
{0, 0.25, 0.25, 0.5}	0.500	1.500	0.500	0.688
{0, 0, 0.4, 0.6}	0.733	0.971	1.029	0.240
{0, 0, 0.3, 0.7}	0.800	0.881	1.119	0.210
{0.16, 0, 0, 0.84}	0.893	0.634	1.366	1.2096
{0, 0, 0.1, 0.9}	0.933	0.469	1.531	0.090
{0, 0, 0.01, 0.99}	0.993	0.081	1.919	0.001
{0, 0, 0, 1.0}	1.000	0.000	2.000	0.000

A difference between the measures arises with respect to scale, where the scale of  $S(P)$  is indexed by domain size, whereas entropy and divergence shift by scale. For example, in an outcome space that consists of  $n = 7$  elements, for a distribution such as  $\{0, 0, 0.2, 0.2, 0.2, 0.2, 0.2\}$  entropy is approximately 2.3 and KL-divergence from the uniform is approximately 0.49. The sharpness score is 1/3, reflecting the degree of concentration over this outcome space. This highlights the distinct properties and uses of these measures: entropy quantifies total uncertainty in terms of the number and spread of possible outcomes, while  $S(P)$  captures the degree of probabilistic concentration over the domain. (However, with regard to the domain transformation properties of  $S(P)$ , see further discussion in Section 5.1.)

Compared to variance,  $S(P)$  provides complementary information by capturing the concentration of mass within the distribution. Distributions with equal variance can differ significantly in sharpness scores, depending on how the mass is concentrated—illustrated in Figure 1. Conversely, variance offers additional insight in cases where sharpness scores are similar but the spatial dispersion of mass within the distribution differs. For example, a high variance combined with a moderate sharpness score reflects a moderately concentrated distribution with two peaks at opposite ends of the domain, while high sharpness and low variance indicate a single-peaked, concentrated distribution. These measures have a natural reciprocal relationship, which is further analyzed in the supplementary material. We also investigate the relationship between entropy and sharpness, showing that they likewise capture complementary aspects of distributional structure. Taken together, the three metrics allow considerably narrowing the range of potential shapes for a given distribution—an advantage that can be useful in model diagnostics and model selection.

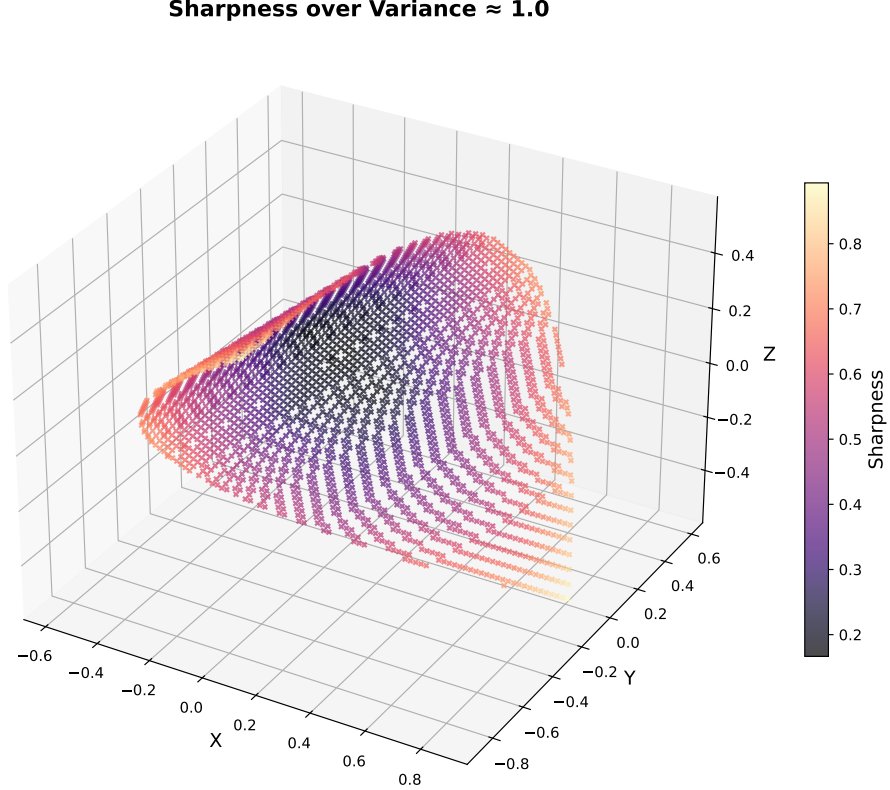


Figure 1: Distributions with approximately equal variance,  $\text{Var}(P) \approx 1.0$ , on the 3-simplex ( $n=4$ ), where each point represents a discrete distribution over four outcomes. Sharpness distinguishes the distributions based on their concentration: sharpness is highest for distributions where mass is heavily concentrated and lowest for diffuse distributions. In this case, a distribution such as  $\{0.19, 0.32, 0.3, 0.19\}$  achieves a low of  $S(P) \approx 0.17$ , while a high of  $S(P) \approx 0.89$  is given by  $\{0.12, 0.02, 0, 0.86\}$ .

### 3.2 Continuous Distributions

We turn next to continuous outcome spaces to evaluate the behavior of  $S(d_*)$ . We examine a set of representative probability density functions defined on the interval  $\Omega = [0, 4]$ , displayed in Table 2.

Table 2: Sharpness score for continuous probability distributions over  $|\Omega| = 4$ . Entropy and KL-divergence from the uniform distribution are expressed in nats.

Distribution	$S(d_*)$	Shannon Entropy	KL-Divergence
$f(y) = 1/ \Omega $	0.000	1.386	0.000
Gaussian: $\mu = 2.8, \sigma = 1$	0.354	1.149	0.237
$f(y) = \frac{1}{Z}[0.5 \varphi(y; 1.2, 0.3^2) + 0.5 \varphi(y; 3.0, 0.4^2)]$	0.459	1.023	0.363
$f(y) = \frac{1}{Z}[0.6 \varphi(y; 1.2, 0.3^2) + 0.4 \varphi(y; 3.0, 0.4^2)]$	0.492	0.977	0.409
Piecewise: 0 on $[0, 2)$ ; 0.5 on $[2, 4]$	0.500	0.693	0.693
Gaussian: $\mu = 2.8, \sigma = 0.5$	0.610	0.690	0.696
Piecewise: 0 on $[0, 2)$ ; 0.15 on $[2, 3)$ ; 0.85 on $[3, 4]$	0.675	0.423	0.964
Gaussian: $\mu = 2.8, \sigma = 0.1$	0.920	-0.884	2.270
Gaussian: $\mu = 2.8, \sigma = 0.01$	0.992	-3.186	4.573
$\delta(y - 2.8)$ (Dirac delta)	1.000	—	—

Similarly to the discrete case,  $S(d_*)$  reflects proportionally increases in concentration of probability mass. It rewards concentration anywhere within the distribution, favoring greater concentration over narrower regions of the domain. This enables the measure, for example, to distinguish between similar piecewise and Gaussian densities, where it rewards the Gaussian density over the piecewise density given its increased concentration at the center point of the distribution. In contrast to Shannon entropy and KL-divergence, the measure provides an interpretable metric of concentration, where the scale of the measure moves between maximal diffusion (0) and maximal concentration (1).

### 3.3 Sharpness in Multidimensional Predictive Settings

To demonstrate the behavior of the continuous sharpness measure in multidimensional cases, we evaluate  $S(d_*)$  for a simplistic example distribution defined over the three-dimensional

unit cube  $\Omega = [0, 1]^3$ . The uniform distribution over the cube is defined by:

$$f_U(x, y, z) = 1, \quad \text{for } (x, y, z) \in \Omega.$$

This distribution places equal weight over all outcomes, representing maximum uncertainty over the domain, thus achieving the minimum sharpness score,  $S(f_U) = 0$ . To contrast with the uniform case, we construct a density that places 99% of the probability mass uniformly within one octant—specifically, the subcube  $[0, 0.5]^3$ —and distributes the remaining 1% evenly across the other seven octants. This yields the following piecewise-constant probability density function:

$$f_{0.99}(x, y, z) = \begin{cases} \frac{0.99}{(0.5)^3} = 7.92, & \text{if } x, y, z \in [0, 0.5], \\ \frac{0.01}{(0.5)^3 \cdot 7} \approx 0.011429, & \text{otherwise.} \end{cases}$$

This density strongly concentrates mass in a localized region of the outcome space, suppressing the majority of the domain. Using a minimal discretization of the domain, we compute:

$$S(f_{0.99}) = 0.865,$$

which reflects the proximity of the predictive distribution to excluding 7/8 of the possible outcome space.  $S(d_*)$  is thus also applicable in multidimensional cases.

## 4 Geometric Properties

We turn next to the geometric properties of the sharpness measure. The sharpness measure induces a natural geometry over a functional representation of the outcome space, where sharpness is represented as a shift away from uniformity and towards increasing concentration. The geometric properties highlight the analytical flexibility of the measure, as well as demonstrating its grounding in a well-defined geometric framework.

## 4.1 Mass-Length Functional Representation

We first examine the mass-length functional version of  $S(d_*)$ , introduced in Section 2.2. This formulation represents sharpness as the area between two curves, where increasing sharpness is reflected in a widening area between the curves—illustrated in Figure 2. Although the measure captures deviation from uniformity, the uniform baseline is not explicitly referenced in the formula (Equation 2.5). Instead, the mass-length representation encodes uniformity and maximal concentration as structural extremes in the rearranged outcome space.

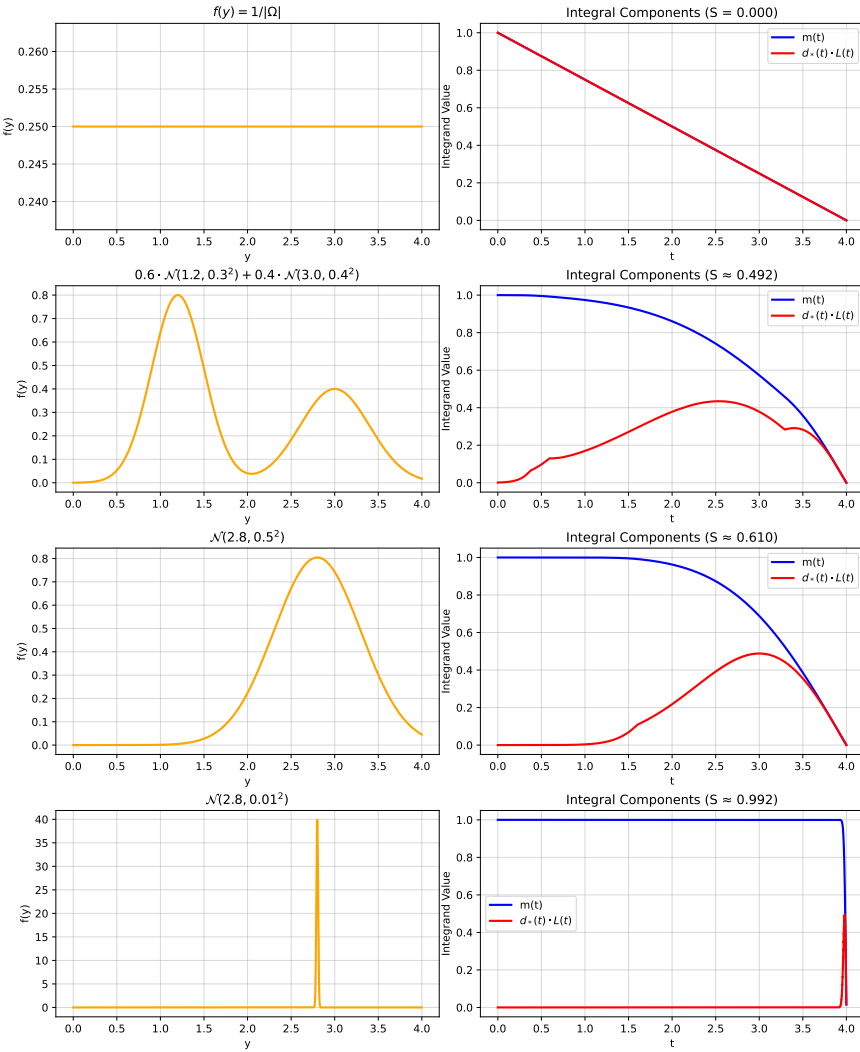


Figure 2: Plots for some of the pdfs in Table 2 and the integral components of  $S(d_*)$ .

The mass-length functional form enables a full decomposition of the sharpness score, where

the composition of the score can be examined region by region. Additionally, while the non-decreasing rearrangement  $d_*$  eliminates spatial information from the original domain, we can still recover points or regions  $y_p \in \Omega$  of interest from the original distribution and represent these meaningfully within the mass-length functional space. For a given point  $y_p$ , its rearranged position  $t_p \in [0, |\Omega|]$  can be approximately recovered by matching its original density value to the rearranged profile:

$$t_p = t_j \quad \text{where} \quad j = \arg \min_i |d_*(t_i) - d(y_p)|.$$

This is best achieved using a fine-grained discretization  $\{y_i\}_{i=1}^N$  of the original distribution (e.g.,  $N = 10,000$ ). In cases where multiple points in the original distribution have the same density, the mapping is non-unique, but for equal density regions, both curves move linearly and in parallel within the mass-length functional space, so the rank of the density can still be recovered (further discussion and illustrations on this point are provided in the supplementary material).

This mapping enables further analysis in the rearranged space, alongside the global sharpness measure. For example, consider that we are interested in examining the allocation of probability mass to certain extreme values. To assess this, we discretize the subregion of interest,  $A \subseteq \Omega$ , as a finite set  $\{y_i\}_{i=1}^M \subset A$  and evaluate the corresponding density values  $d(y_i)$ . We then identify the minimal positive density in the full domain,

$$d_{\min} = \min \{d(y) \mid y \in \Omega, d(y) > 0\},$$

and locate any points in  $A$  that satisfy  $d(y_i) \geq d_{\min}$ . To then recover these points in the rearranged domain, we map each point  $y_i \in A$  with nonzero density to its corresponding location  $t_i \in [0, |\Omega|]$  using the above recovery formula. For further reference, the location  $y_{\min} \in \Omega$  where  $d(y_{\min}) = d_{\min}$  can be used to identify the boundary between supported and

excluded regions. In the rearranged space, the value

$$t_{\min} = t_{j_{\min}}, \quad \text{where} \quad j_{\min} = \arg \min_i |d_*(t_i) - d_{\min}|,$$

marks the extent of the rearranged domain where  $d(y) = 0$ . This mapping structure is illustrated in Figure 3 for a domain of length  $\Omega = 8$  and where we explore whether the original distribution included non-zero values within the range  $[5, 8]$ .

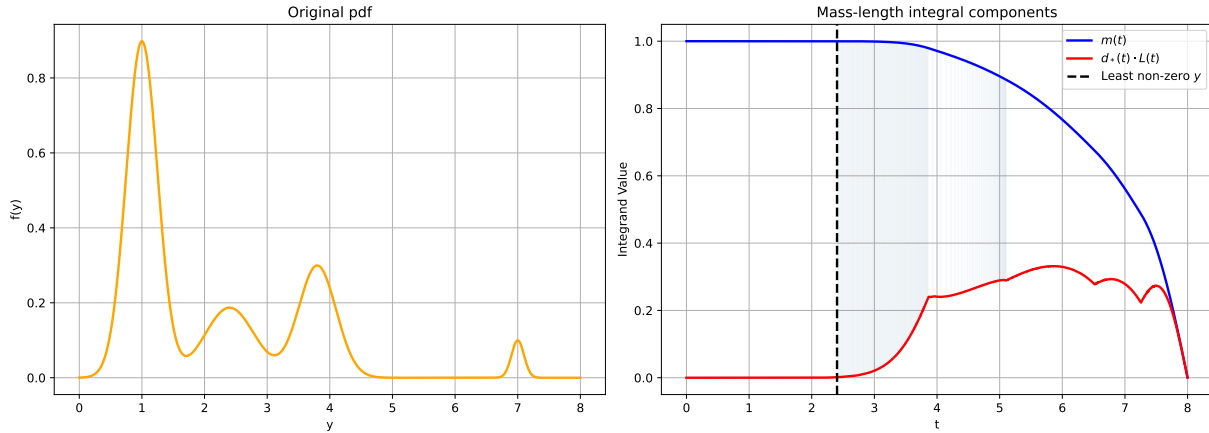


Figure 3: The original probability density function is shown on the left. On the right, the rearrangement of this density is represented in the mass-length functional space, with the non-zero probabilities within the range  $[5, 8]$  represented by the lines between the curves. By examining the relative location and the mass curve above the lines, we can further observe their relative rank as well as the amount of probability mass that was assigned to higher density regions.

This representation enables examining several quantities of interest—such as relative rank and mass above a density threshold—within the rearranged space for given points or areas within the original distribution (e.g., mean, median, observed value), and can provide a convenient analysis method with complex, multidimensional distributions. Formulas for computing several relevant quantities are provided in the supplementary material of this article.

## 4.2 Mass Displacement and Curvature

The simplified expression of the sharpness measure, derived in Section 2.2, further illustrates the mathematical properties of the measure. In its simplified form, the sharpness measure,

$$S(d_*) = \frac{2}{|\Omega|} \int_0^{|\Omega|} t \cdot d_*(t) dt - 1,$$

represents the expectation of  $t$  under the non-decreasing rearrangement  $d_*(t)$  of the original distribution  $d$ . The rearrangement orders the probability mass by magnitude, so that increasing concentration corresponds to a shift of mass toward larger  $t$ -values, thereby increasing the mean. This is shown in Figure 4.

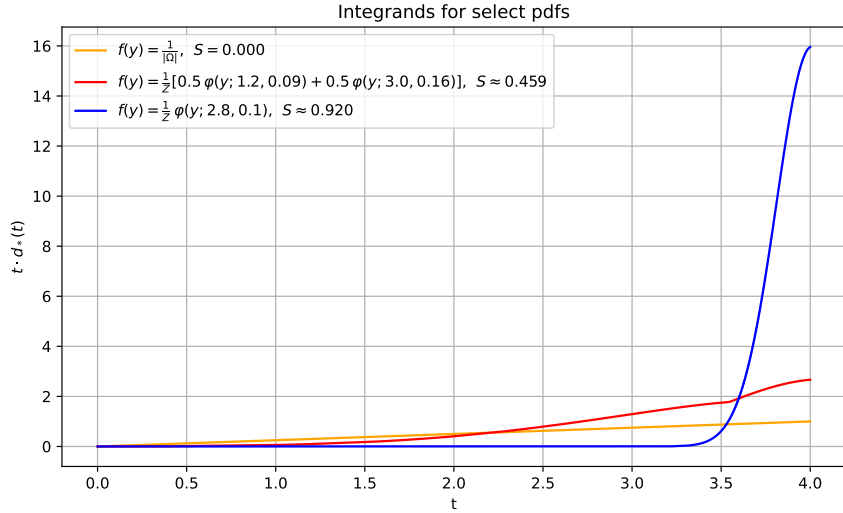


Figure 4: Plots of the integrands for three of the pdfs in Table 2 using the simplified  $S(d_*)$  formula.

This representation shows how increased concentration of probability mass leads to a higher sharpness score: any redistribution of mass toward greater values increases the mean, and thereby the sharpness score.

### 4.3 A Gini-Style Representation

We observe that  $S(d_*)$  admits a natural interpretation as a Gini-type coefficient applied to the predictive distribution. The classical Gini coefficient is given by  $G = 1 - 2 \int_0^1 L(p) dp$ , where the Lorenz curve is defined as  $L(p) = \mu^{-1} \int_0^p F^{-1}(t) dt$ ,  $\mu$  is the population mean, and  $F^{-1}(t)$  denotes the quantile function of the income distribution (Gastwirth 1972, Kakwani 1980). In our context, probability mass replaces income, and the Lorenz-type curve measures the cumulative share of total probability mass accumulated in fractions of the rearranged domain.

Let  $d_*: [0, |\Omega|] \rightarrow \mathbb{R}_{\geq 0}$  be the non-decreasing rearrangement of a predictive density  $d$  defined over a bounded domain  $\Omega \subset \mathbb{R}$ . Define the cumulative mass function  $F(t) = \int_0^t d_*(s) ds$ , and let  $u = t/|\Omega| \in [0, 1]$  denote the normalized domain. The Lorenz-type curve over this rearranged space is given by

$$L(u) = \int_0^{u|\Omega|} d_*(s) ds, \quad (4.1)$$

which measures the proportion of total probability mass below the  $u$ -quantile of the rearranged outcome space.

Using the simplified sharpness expression (Equation 2.6) and applying the change of variables  $t = u|\Omega|$ , with  $dt = |\Omega| du$ , we obtain:

$$S(d_*) = 2|\Omega| \int_0^1 u d_*(u|\Omega|) du - 1.$$

Noting that  $L'(u) = \frac{d}{du} \int_0^{u|\Omega|} d_*(s) ds = d_*(u|\Omega|) \cdot |\Omega|$ , it follows that  $d_*(u|\Omega|) = \frac{1}{|\Omega|} L'(u)$ , and thus:

$$S(d_*) = 2 \int_0^1 u L'(u) du - 1.$$

Applying integration by parts,

$$\int_0^1 u L'(u) du = [uL(u)]_0^1 - \int_0^1 L(u) du = 1 - \int_0^1 L(u) du,$$

since  $L(1) = \int_0^{|\Omega|} d_*(s) ds = 1$ . Substituting gives

$$\begin{aligned} S(d_*) &= 2(1 - \int_0^1 L(u) du) - 1 \\ &= 1 - 2 \int_0^1 L(u) du. \end{aligned} \quad (4.2)$$

Hence, the sharpness functional is equivalent to a Gini-style coefficient applied to the rearranged predictive distribution. This expression allows representing predictive sharpness similarly to the Gini coefficient, which is illustrated in Figure 5.

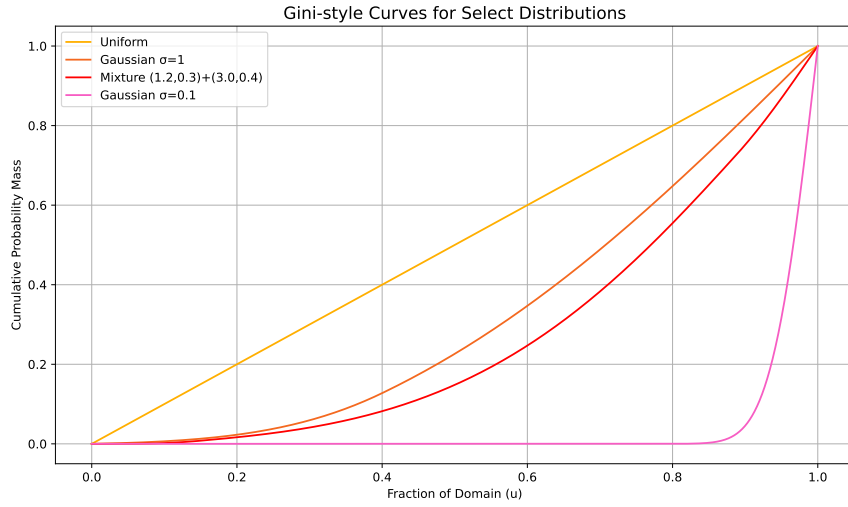


Figure 5: A Gini-style representation of the uniform and three of the pdfs in Table 2.

The Gini-style representation provides a visually intuitive means of comparing the predictive sharpness of different distributions defined over the same domain. However, we note that the Gini-type version is computationally less efficient than the simplified equation 2.6, and we further lose the decomposition and analytical features of the mass-length functional form (Equation 2.5). As such, within the probabilistic context, its practical utility lies chiefly in visualizations, rather than in diagnostic or computational applications. Nonetheless, we may further observe that given the mathematical equivalency between the three formulas, the traditional Gini coefficient by implication can be expressed similarly as the mass-length functional of probabilistic sharpness. Here, the total remaining share of wealth again replaces

the total remaining probability mass, and  $d_*$  is replaced by the rank of wealth by quantile of the population, sorted from smallest to largest. This provides access to the analytical tools provided by the mass-length functional form, including a regional decomposition focused on the low income side (Section 4.1), and constitutes an area for further exploration.

## 4.4 Conclusion

The sharpness measure  $S(d_*)$ , while formally defined through integrals over rearranged densities, admits a rich geometric interpretation. The formula measures how far probability mass is shifted from uniformity toward more concentrated regions, and visualizes this shift as a form of mass displacement or curvature. This offers a geometrically grounded framework for exploring probabilistic concentration over outcome spaces.

# 5 Applications

The sharpness measure is designed to quantify a specific property of a probabilistic forecast—the extent to which it concentrates over subsets of the outcome space. In this section, we discuss applications of the measure in model diagnostics.

## 5.1 Disentangling Sharpness from Accuracy and Calibration

In probabilistic modeling, proper scoring rules such as CRPS ([Matheson & Winkler 1976](#)) provide a commonly used and convenient tool for jointly assessing calibration and sharpness ([Gneiting & Raftery 2007](#), [Gneiting & Katzfuss 2014](#), [Arnold et al. 2024](#)). However, a precise treatment of sharpness as an independent quantity can provide additional diagnostic insight. For example, two predictive models may achieve comparable scores under a proper scoring rule but differ in how narrowly they concentrate probability mass versus how well they reflect the actual empirical frequencies. Reporting sharpness as an independent measure

helps reveal these differences, while also offering an interpretable metric for how tightly the models have concentrated their predictions over the given domain. Moreover, supporting practical applications, the sharpness measure can be readily computed for single probabilistic forecasts, averaged across multiple cases, as well as used in pre-observational evaluation and comparisons.

In contexts where calibration and sharpness are assessed separately, the sharpness measure can be applied alongside calibration diagnostics such as the probability integral transform (PIT). The PIT evaluates the consistency between predictive distributions and observed outcomes by transforming each observation through its corresponding cumulative distribution function (CDF); under probabilistic calibration, the resulting PIT values should be uniformly distributed (Gneiting et al. 2007, Gneiting & Katzfuss 2014). While the PIT provides insight into systematic miscalibration—such as bias, overdispersion, or underdispersion—it does not assess the informativeness or concentration of the forecasts (Gneiting et al. 2007). The sharpness measure addresses this gap by quantifying how narrowly the forecast distribution concentrates mass, independent of observed outcomes. Used together, PIT and sharpness offer a more complete picture: they help distinguish models that are well-calibrated but diffuse and uninformative relative to the overall domain, and those that may be sharply focused but yet poorly calibrated. This separation supports more targeted model diagnostics, refinement, and evaluation by providing a clearly interpretable view of both calibration and sharpness.

In individual cases—for example, identifying outliers within an ensemble forecast (e.g., detection of cases where ensemble members are confident but wrong)—the sharpness measure can be combined with a measure of accuracy to yield complementary insight. When applied together with the proposed sharpness measure, relative likelihood provides one option for

this purpose. Relative likelihood is defined by

$$\text{RL}(y_{\text{obs}}) = \frac{d(y_{\text{obs}})}{\max_{y \in \Omega} d(y)}, \quad (5.1)$$

with values near 1 indicating that the observation occurred at or near a mode of the distribution.

To illustrate this joint framework, consider a renormalized Gaussian distribution with mean  $\mu = 3.4$ , standard deviation  $\sigma = 0.8$ , and support restricted to  $\Omega = [0, 5]$ . This predictive distribution yields a sharpness score of approximately  $S(d_*) \approx 0.516$ . For an observed outcome such as  $y_{\text{obs}} = 2.0$ , the relative likelihood is  $\text{RL}(2.0) \approx 0.216$ , indicating that the model placed substantially more mass elsewhere in the domain. By contrast, for  $y_{\text{obs}} = 3.5$ , we obtain  $\text{RL}(3.5) \approx 0.992$ , indicating that the model was concentrated around the correct value. However, the meaningfulness of this match is subject to the sharpness of the forecast, and the value is thus best interpreted with reference to the sharpness measure (see Figure 6) (for example, relative likelihood would be 1 for all outcomes under the uniform distribution, but the minimal sharpness score reveals that such high likelihood in this case is meaningless). By setting threshold values for each measure, they can be tailored for tracking cases of interest; for example, forecasts that assigned mass to an observed value but are too diffuse to be informative, or forecasts that are confident yet miss the target.

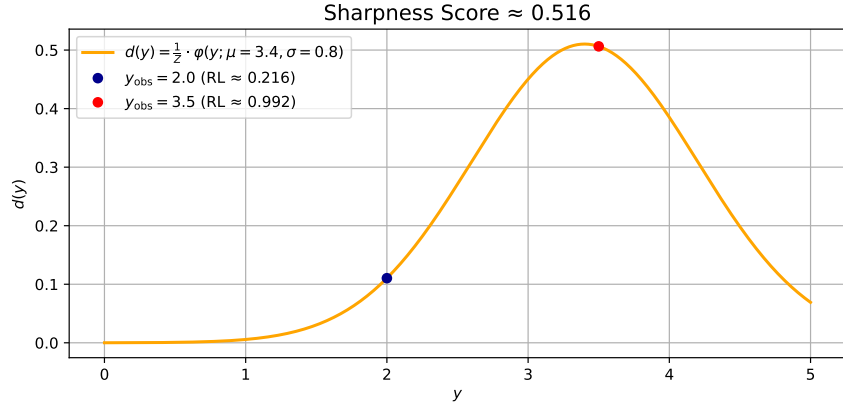


Figure 6: The sharpness score and relative likelihood for two observed values.

In practical applications, the sharpness score is scaled by the choice of domain. When an outcome variable lies on a well-defined, bounded scale, domain choice is straightforward. In other cases, where extreme values are physically possible but exceedingly improbable (for example, such as those found in weather forecasting), the relevant domain may be defined over a theoretically relevant or a practically meaningful range. In all cases, the interpretation of the sharpness scores is context-dependent: although the sharpness measure has definite, clearly interpretable endpoints, what qualifies as a “sharp” forecast in between is benchmarked against the concentration typically achieved by models in the given domain (Thompson & Skau 2023). Accordingly, sharpness scores are best interpreted comparatively, with reference to established benchmarks within a given application domain.

However, we note that as long as the same quantity is being measured and the overall domain is bounded, the specific choice of the domain size for a given application matters only for scaling the sharpness measure, not for the intrinsic sharpness score of the distribution defined over the full domain range (where the sharpness measure ranges between the uniform distribution and deterministic point prediction). Any valid probability distribution that is defined over a subregion of a particular domain assigns, by definition, zero probability to the excluded regions. Consequently, for both the discrete and continuous cases, we can recover

the sharpness score under an expanded definition of the domain (up until the full domain range), or compute it under a restricted definition that omits certain zero-probability regions. The measure can thus be effectively rescaled to focus only on the support of a distribution for arbitrary, bounded domains, while alternative truncation schemes of zero-probability regions yield, via transformation formulas, fully comparable sharpness scores for any valid distributions. The corresponding transformation formulas for rescaling sharpness scores to extended and restricted definitions of a particular domain are provided below in Table 3, and the derivation of the formulas is provided in the supplementary material:

Table 3: Sharpness score (S) transformations across domains.

Transformation	Formula
Forward (Discrete): embed from size $m$ to size $n > m$	$S_n = 1 + \frac{m-1}{n-1}(S_m - 1)$
Inverse (Discrete): restrict from size $n$ to size $m < n$	$S_m = 1 + \frac{n-1}{m-1}(S_n - 1)$
Forward (Continuous): extend from measure $\ell$ to $L > \ell$	$S_L = 1 + \left(\frac{\ell}{L}\right)(S_\ell - 1)$
Inverse (Continuous): restrict from measure $L$ to $\ell < L$	$S_\ell = 1 + \left(\frac{L}{\ell}\right)(S_L - 1)$

For practical computation, it is recommended to use the simplified expressions of both the discrete and continuous sharpness measures (Equations 2.4 and 2.6, respectively). A Python implementation of all the measures and formulas introduced in this paper is provided in the accompanying material.

## 5.2 Sharpness Diagnostics for Spatial Forecasts

To illustrate the sharpness functional  $S(d_*)$  in a forecasting setting, we simulate rainfall ensemble predictions over a  $6 \times 6$  spatial grid. Each grid cell contains a predictive distribution based on 30 ensemble members, representing rainfall forecasts in millimeters within a given interval  $[0, 10]$ . For each cell, the underlying distribution is produced using a normal

distribution with a mean randomly selected from the set  $\{0.2, 0.5, 1.0, 2.0, 3.0\}$  with probabilities  $\{0.4, 0.3, 0.15, 0.1, 0.05\}$  and a standard deviation drawn uniformly from the interval  $[0.1, 1.0]$ . From this distribution, thirty samples were drawn for each cell representing the ensemble forecast.

To represent the ensemble forecasts for each cell, we use a histogram with 50 equal-width bins over  $[0, 10]$ , normalized to produce a piecewise constant probability density function. (For this application, kernel density estimation using Scott's rule and a reflection correction near domain boundaries yielded very similar results.) This density is then rearranged into its non-decreasing form  $d_*(t)$ , and the sharpness functional  $S(d_*)$  is computed numerically via a Riemann sum approximation. For each cell, we report the sharpness score  $S(d_*)$  and the 90% confidence interval for reference, shown in Figure 7.

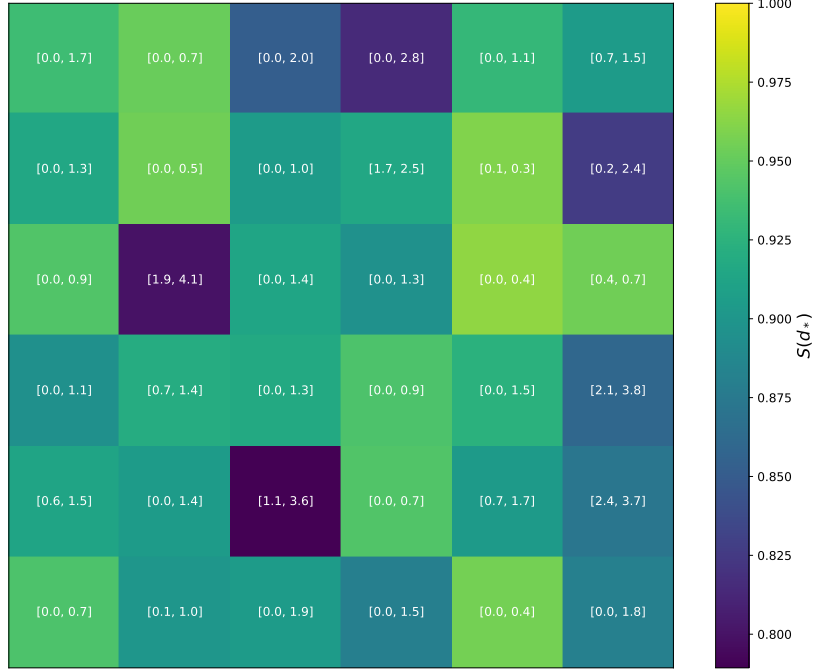


Figure 7: An illustration of predictive sharpness in ensemble rainfall prediction over a 6x6 spatial grid. The sharpness score encodes the concentration of the ensemble forecast for each cell. Despite similar confidence intervals, the concentration of the forecasts may differ. For example, while cells 1,3 and 3,2 have similar 90% confidence intervals, the former cell has a higher sharpness score, indicating a more narrowly concentrated distribution within that cell and a more diffuse distribution within the latter.

This type of visualization facilitates detailed spatial comparisons, revealing grid-by-grid differences. Computing the measure over successive updates of the forecast enables tracking how sharpness evolves in each grid cell over time, thus helping identify trends, outliers (e.g., aberrant concentration or diffusion within cells), emerging areas of forecast confidence, or zones of increasing diffusion.

## 6 Discussion

The predictive sharpness measure introduced in this paper offers a principled method for quantifying how much a probabilistic prediction concentrates over an outcome space. The measure focuses on the structure of the predictive distribution itself—specifically, the extent to which it concentrates probability mass over narrower subsets of the domain. The measure offers a distinct perspective from conventional tools such as scoring rules, entropy, or divergence measures, focusing specifically on probabilistic concentration.

Further applications of the measure include model comparison and selection, Bayesian analysis, and hypothesis evaluation. In Bayesian analysis, for example, the measure offers a tool for assessing the informativeness of prior and posterior distributions, as well as quantifying relative gains from prior to posterior. The measure may be particularly suited for use in objective Bayesian frameworks, where priors are often chosen to reflect minimal information, generally, the uniform distribution in bounded domains (Williamson 2010). In model selection, the measure could be utilized, for example, as a regularizing component: models may be penalized for excessive confidence or rewarded for producing appropriately narrow predictions. In the supplementary material to this article, we discuss how the measure can be combined with either entropy or variance to select for highly specific distribution shapes. More broadly, the sharpness measure may also be applied in hypothesis and theory evaluation, both to assess a theory’s predictive sharpness as such as well as examining the extent to which a hypothesis has placed itself under risk by constraining possibility spaces—an area of hypothesis evaluation that has attracted recent interest (Thompson & Skau 2023, van Dongen et al. 2023, Syrjänen in press).

Further extensions of the framework, including treatment of unbounded or structured domains and covariate-dependent predictions warrant future development. The current measure is defined for bounded domains, where normalization and geometric interpretation

are straightforward. Extending the measure to unbounded spaces requires additional structure, such as truncation schemes (e.g., at a high quantile of cumulative mass), decay rate constraints, or a reference-based definition based on a restricted domain size. For example, in the latter case, one possibility is to define the domain over a theoretically plausible range and quantify the sharpness of alternative distributions relative to this baseline. Developing a principled extension along these lines remains an area for future work.

In summary, the predictive sharpness measure captures a foundational yet under-theorized dimension of probabilistic prediction: the degree to which a prediction concentrates over the outcome space. By quantifying this concentration in a scale-free, interpretable, and geometrically grounded manner, the measure fills a gap in the toolkit for model evaluation and prediction assessment. It complements existing measures of calibration and uncertainty, and opens new avenues for evaluating, comparing, and refining probabilistic models.

**Reproducibility Statement:** A Python implementation of the formulas defined in this paper and the Python scripts for reproducing all tables, figures, simulations, and experiments within the paper is available at: <https://github.com/psyrjane/Predictive-sharpness>.

## References

Arnold, S., Walz, E. M., Ziegel, J. & Gneiting, T. (2024), ‘Decompositions of the mean continuous ranked probability score’, *Electronic Journal of Statistics* **18**, 4992–5044.

Du, H. (2021), ‘Beyond strictly proper scoring rules: The importance of being local’, *Weather and Forecasting* **36**, 457–468.

Gastwirth, J. L. (1972), ‘The estimation of the lorenz curve and gini index’, *The Review of Economics and Statistics* **54**, 306–316.

Gneiting, T., Balabdaoui, F. & Raftery, A. E. (2007), ‘Probabilistic forecasts, calibration and sharpness’, *Journal of the Royal Statistical Society Series B: Statistical Methodology* **69**, 243–268.

Gneiting, T. & Katzfuss, M. (2014), ‘Probabilistic forecasting’, *Annual Review of Statistics and Its Application* **1**, 125–151.

Gneiting, T. & Raftery, A. E. (2007), ‘Strictly proper scoring rules, prediction, and estimation’, *Journal of the American Statistical Association* **102**, 359–378.

Kakwani, N. C. (1980), *Income Inequality and Poverty: Methods of Estimation and Policy Applications*, World Bank, New York.

Matheson, J. E. & Winkler, R. L. (1976), ‘Scoring rules for continuous probability distributions’, *Management Science* **22**, 1087–1096.

Syrjänen, P. (in press), ‘Dimensions of predictive success’, *The British Journal for the Philosophy of Science* .

Thompson, W. H. & Skau, S. (2023), ‘On the scope of scientific hypotheses’, *Royal Society Open Science* **10**, 230607.

van Dongen, N., Sprenger, J. & Wagenmakers, E.-J. (2023), ‘A bayesian perspective on severity: risky predictions and specific hypotheses’, *Psychonomic Bulletin and Review* **30**, 516–533.

Williamson, J. (2010), *In Defence of Objective Bayesianism*, Oxford University Press, Oxford.

## SUPPLEMENTARY MATERIAL

Section [S1](#) provides proofs of mathematical properties.

Section [S2](#) derives formulas for sharpness score transformations across discrete and continuous domains.

Section [S3](#) derives formulas for analysis in the rearranged space, including local contributions to sharpness score and recovery of key points.

Section [S4](#) investigates relationships between sharpness, entropy, and variance.

## S1 Proofs

We examine formal properties of the continuous sharpness measure  $S(d_*)$ . We focus on desirable mathematical characteristics, including normalization and monotonicity.

### S1.1 Normalization

The measure should lie within the closed unit interval  $[0, 1]$ , with 0 corresponding to a maximally vague (uniform) prediction and 1 corresponding to a maximally sharp prediction. We show that  $S(d_*)$  satisfies this requirement and attains the endpoint values in appropriate limiting cases.

**Theorem S1.1** (Normalization of  $S(d_*)$ ). *Let  $\Omega \subset \mathbb{R}$  be a bounded, measurable domain with finite Lebesgue measure  $|\Omega| < \infty$ , and let  $d: \Omega \rightarrow \mathbb{R}_{\geq 0}$  be a probability density function such that  $\int_{\Omega} d(y) dy = 1$ . Then the continuous predictive sharpness measure  $S(d_*)$  satisfies:*

$$0 \leq S(d_*) \leq 1.$$

Equality is achieved at the lower bound if and only if  $d$  is the uniform distribution over  $\Omega$ , and the upper bound is approached in the limit as  $d$  converges to a Dirac delta function.

*Proof.* We begin with the simplified formula derived in Section 2.2 of the article:

$$S(d_*) = \frac{2}{|\Omega|} \int_0^{|\Omega|} t d_*(t) dt - 1,$$

where  $d_*(t)$  is the non-decreasing rearrangement of  $d$ . We now determine the bounds of this expression. Since  $d_*$  is a non-negative function on  $[0, |\Omega|]$  with total integral 1, the quantity  $\int_0^{|\Omega|} t d_*(t) dt$  represents the expectation of  $t$  under  $d_*$ . This expectation is minimized when  $d_*(t)$  is uniform on  $[0, |\Omega|]$ , i.e.,  $d_*(t) = \frac{1}{|\Omega|}$ , because any non-uniform, non-decreasing rearrangement shifts more probability mass toward higher values of  $t$ , thus increasing the mean. Hence,

$$\int_0^{|\Omega|} t d_*(t) dt \geq \int_0^{|\Omega|} t \cdot \frac{1}{|\Omega|} dt = \frac{1}{|\Omega|} \cdot \frac{|\Omega|^2}{2} = \frac{|\Omega|}{2},$$

with equality if and only if  $d_*$  is uniform. Substituting this into the formula gives:

$$S(d_*) \geq \frac{2}{|\Omega|} \cdot \frac{|\Omega|}{2} - 1 = 0.$$

To examine the maximum, consider the limit where  $d_*$  concentrates all mass at the endpoint  $t = |\Omega|$  (i.e.,  $d$  approaches a Dirac delta). For example, let

$$d_*(t) = \frac{1}{\delta} \cdot \mathbf{1}_{[|\Omega|-\delta, |\Omega|]}(t),$$

so that  $d_*$  is a block of height  $1/\delta$  over a short interval of width  $\delta$ .

Then

$$\begin{aligned} \int_0^{|\Omega|} t d_*(t) dt &= \frac{1}{\delta} \int_{|\Omega|-\delta}^{|\Omega|} t dt = \frac{1}{\delta} \cdot \left[ \frac{t^2}{2} \right]_{|\Omega|-\delta}^{|\Omega|} = \frac{1}{\delta} \cdot \left( \frac{|\Omega|^2}{2} - \frac{(|\Omega|-\delta)^2}{2} \right), \\ &= \frac{1}{2\delta} \cdot (2|\Omega|\delta - \delta^2) = |\Omega| - \frac{\delta}{2} \longrightarrow |\Omega| \quad \text{as } \delta \rightarrow 0. \end{aligned}$$

Hence,

$$S(d_*) \rightarrow \frac{2}{|\Omega|} \cdot |\Omega| - 1 = 1.$$

Therefore,

$$0 \leq S(d_*) \leq 1,$$

with equality at endpoints as claimed.  $\square$

**Remark.** While the Dirac delta function  $\delta(y - y_0)$  is not a member of  $L^1(\Omega)$  and cannot be substituted directly into the definition of  $S(d_*)$ , it is nevertheless instructive to evaluate the sharpness formula symbolically under the assumption that  $d_*(t) = \delta(t - |\Omega|)$ . Then:

$$\int_0^{|\Omega|} t \cdot d_*(t) dt = \int_0^{|\Omega|} t \cdot \delta(t - |\Omega|) dt = |\Omega|,$$

which leads to the symbolic expression:

$$S(d_*) = \frac{2}{|\Omega|} \cdot |\Omega| - 1 = 1.$$

This aligns with the limiting behavior of  $S(d_*)$  under sequences of densities that converge weakly to the Dirac delta, thereby confirming that the formula is consistent with maximal sharpness in the idealized limit.

## S1.2 Monotonicity

We show that the sharpness measure  $S(d_*)$  is strictly increasing when the non-decreasing rearrangement  $d_*(t)$  of one density assigns more probability mass to higher values of  $t \in [0, |\Omega|]$  than another.

**Theorem S1.2** (Monotonicity of  $S(d_*)$ ). *Let  $\Omega \subset \mathbb{R}$  be a bounded, measurable domain with finite measure  $|\Omega| < \infty$ , and let  $d_1, d_2: \Omega \rightarrow \mathbb{R}_{\geq 0}$  be two probability density functions such that  $\int_{\Omega} d_i(y) dy = 1$  for  $i = 1, 2$ . Suppose that their non-decreasing rearrangements  $d_{1*}, d_{2*}$  satisfy:*

$$\int_0^t d_{1*}(s) ds \geq \int_0^t d_{2*}(s) ds \quad \text{for all } t \in [0, |\Omega|],$$

where  $d_{i*}$  denotes the non-decreasing rearrangement of  $d_i$ . Then:

$$S(d_{1*}) \leq S(d_{2*}),$$

with strict inequality if  $d_{1*} \neq d_{2*}$ .

*Proof.* From the simplified formula, sharpness can be written as

$$S(d_*) = \frac{2}{|\Omega|} \mathbb{E}_{d_*}[T] - 1,$$

where  $T$  is a random variable on  $[0, |\Omega|]$  with density  $d_*$ .

Define  $F_i(t) = \int_0^t d_{i*}(s) ds$ , the cumulative distribution function of  $T_i \sim d_{i*}$ , for  $i = 1, 2$ . By assumption,  $F_1(t) \geq F_2(t)$  for all  $t$ . This means  $T_2$  *first-order stochastically dominates*  $T_1$ . A standard property of stochastic dominance is that  $\mathbb{E}[T_1] \leq \mathbb{E}[T_2]$ , with strict inequality if the dominance is strict.

Therefore,

$$S(d_{1*}) = \frac{2}{|\Omega|} \mathbb{E}_{d_{1*}}[T_1] - 1 \leq \frac{2}{|\Omega|} \mathbb{E}_{d_{2*}}[T_2] - 1 = S(d_{2*}),$$

with strict inequality whenever  $d_{1*} \neq d_{2*}$  on a set of positive measure.  $\square$

## S2 Transformations Across Domains

### S2.1 Discrete Case

Let  $S_m$  be the sharpness score of a probability distribution  $P$  defined over  $m$  outcomes. We are interested in the sharpness score  $S_n$  of the same distribution embedded in a larger domain of size  $n > m$  by assigning probability zero to the remaining  $n - m$  outcomes.

#### S2.1.0.1 Forward Transformation (from $m$ to $n$ ):

Given:

- A distribution  $P$  over  $m$  outcomes with sharpness score  $S_m$ .
- A larger domain of size  $n > m$ , where  $k = n - m$  additional outcomes are assigned probability zero.

We find the sharpness score  $S_n$  of  $P$  defined over the size- $n$  domain. The sharpness score of a distribution  $P = \{p_1, \dots, p_n\}$  over a domain of size  $n$  is given by:

$$S(P) = \frac{1}{n-1} \sum_{j=1}^{n-1} (m_{(j)} - p_{(j)} L_{(j)}),$$

where

- the probabilities  $p_{(j)}$  are sorted in ascending order
- $m_{(j)} = \sum_{k=j}^n p_{(k)}$  is the tail mass from position  $j$  onward
- $L_{(j)} = n - j + 1$  is the number of remaining outcomes from position  $j$  onward.

To embed the original distribution into the larger domain, we create:

$$P' = \underbrace{\{0, 0, \dots, 0\}}_{k \text{ zeros}}, p_1, \dots, p_m$$

For each of the  $k$  zeros:

$$p_{(j)} = 0, \quad m_{(j)} = 1, \quad L_{(j)} = n - j + 1 \Rightarrow m_{(j)} - p_{(j)} \cdot L_{(j)} = 1$$

So the total contribution from the  $k$  zeros is:

$$\sum_{j=1}^k 1 = k$$

The sharpness score  $S_m$  was originally defined as:

$$S_m = \frac{1}{m-1} \sum_{j=1}^{m-1} (m_{(j)} - p_{(j)} L_{(j)})$$

Multiplying by  $m - 1$ , we recover the total unnormalized contribution to the sharpness score:

$$\text{Contribution} = (m - 1)S_m$$

This total is reused as-is in the expanded domain—we are simply changing the normalization from  $m - 1$  to  $n - 1$ . To find  $S_n$ , we combine the contributions from  $k = n - m$  and  $(m - 1)S_m$ :

$$\begin{aligned} S_n &= \frac{(n - m) + (m - 1)S_m}{n - 1} \\ &= \frac{(n - 1) - (m - 1) + (m - 1)S_m}{n - 1} \\ &= \frac{(n - 1) + [(m - 1)S_m - (m - 1)]}{n - 1} \\ &= \frac{(n - 1) + (m - 1)(S_m - 1)}{n - 1} \\ &= 1 + \frac{(m - 1)(S_m - 1)}{n - 1} \end{aligned}$$

Therefore, the forward transformation is:

$$S_n = 1 + \frac{m - 1}{n - 1}(S_m - 1)$$

This formula gives, for arbitrary domains of size  $n$  and  $m$  (where  $n > m$ ) and the sharpness score  $S_m$  of a discrete probability distribution  $P$  defined over  $m$ , the sharpness score  $S_n$  of  $P$ .

**S2.1.0.2 Inverse Transformation (from  $n$  to  $m$ ):** Let  $P$  be a probability distribution over  $n$  outcomes with sharpness score  $S_n(P)$ , and let  $m < n$  denote a smaller outcome set. Suppose that  $P$  assigns zero probability to at least  $n - m$  of the  $n$  outcomes. We begin with the forward transformation formula:

$$S_n = 1 + \frac{(m - 1)(S_m - 1)}{n - 1}$$

To recover  $S_m$ , we rearrange the expression:

$$\begin{aligned}
 S_n - 1 &= \frac{(m-1)(S_m - 1)}{n-1} \\
 (n-1)(S_n - 1) &= (m-1)(S_m - 1) \\
 S_m - 1 &= \frac{(n-1)(S_n - 1)}{m-1} \\
 S_m &= 1 + \frac{(n-1)(S_n - 1)}{m-1}
 \end{aligned}$$

Therefore, the inverse transformation is:

$$S_m = 1 + \frac{n-1}{m-1}(S_n - 1)$$

The inverse operation reverses the shift added by the zeros and rescales the result from normalization over  $(n-1)$  to normalization over  $(m-1)$ . Thus, this formula expresses, given arbitrary domains of size  $n$  and  $m$  (with  $n > m$ ) and the sharpness score  $S_n(P)$  of a discrete distribution  $P$  defined over  $n$  outcomes, the sharpness score  $S_m(P)$  of the same distribution restricted to the smaller domain of size  $m$ , on the assumption that the  $n-m$  additional outcomes are assigned zero probability. The inverse transformation formula enables computing sharpness score over a subdomain of interest by truncating zero-probability outcomes and rescaling accordingly.

## S2.2 Continuous Case

Let  $d$  be a probability density function defined over a measurable domain  $A \subset \mathbb{R}^n$  with Lebesgue measure  $\ell = \lambda(A)$ , and let  $S_\ell$  denote its sharpness score over this domain. We are interested in the sharpness score  $S_L$  of  $d$  extended to a larger domain  $B \supset A$ , where  $\lambda(B) = L > \ell$ , and  $d(y) = 0$  for all  $y \in B \setminus A$ .

### S2.2.0.1 Forward Transformation (from $\ell$ to $L$ ):

Let  $d: A \rightarrow \mathbb{R}_{\geq 0}$  be a probability density function defined over a measurable domain  $A \subset \mathbb{R}^n$  and let  $\ell = \lambda(A)$  denote its Lebesgue measure, satisfying

$$\int_A d(y) dy = 1.$$

Let  $d_*(t)$  denote the non-decreasing rearrangement of  $d$  over  $[0, \ell]$ , and let  $S_\ell$  be its sharpness score over  $\ell$ .

To embed  $d$  in a larger domain  $B \subset \mathbb{R}^n$  with  $\lambda(B) = L > \ell$ , define the extended density  $\tilde{d}: B \rightarrow \mathbb{R}_{\geq 0}$  by:

$$\tilde{d}(y) = \begin{cases} d(y), & y \in A, \\ 0, & y \in B \setminus A. \end{cases}$$

Then  $\tilde{d}$  is a valid probability density on  $B$  with:

$$\int_B \tilde{d}(y) dy = \int_A d(y) dy = 1.$$

Let  $\tilde{d}_*(t): [0, L] \rightarrow \mathbb{R}_{\geq 0}$  denote the non-decreasing rearrangement of  $\tilde{d}$ . Since  $\tilde{d}(y) = 0$  on the set  $B \setminus A$ , which has measure  $L - \ell$ , the rearrangement satisfies:

$$\tilde{d}_*(t) = \begin{cases} 0, & t \in [0, L - \ell], \\ d_*(t - (L - \ell)), & t \in (L - \ell, L]. \end{cases}$$

The sharpness score over the larger domain is defined as:

$$S_L = \frac{2}{L} \int_0^L t \cdot \tilde{d}_*(t) dt - 1.$$

Substituting the piecewise definition of  $\tilde{d}_*$ , we have:

$$S_L = \frac{2}{L} \left( \int_0^{L-\ell} t \cdot 0 dt + \int_{L-\ell}^L t \cdot d_*(t - (L - \ell)) dt \right) - 1.$$

Change variables in the second integral by letting  $u = t - (L - \ell)$ , so  $t = u + (L - \ell)$ , and  $u \in [0, \ell]$ . Then:

$$S_L = \frac{2}{L} \int_0^\ell (u + (L - \ell)) \cdot d_*(u) du - 1.$$

Distribute and split the integral:

$$S_L = \frac{2}{L} \left( \int_0^\ell u \cdot d_*(u) du + (L - \ell) \int_0^\ell d_*(u) du \right) - 1.$$

Since  $\int_0^\ell d_*(u) du = 1$ , we get:

$$S_L = \frac{2}{L} \left( \int_0^\ell u \cdot d_*(u) du + (L - \ell) \right) - 1.$$

From the definition of  $S_\ell$ , we have:

$$S_\ell = \frac{2}{\ell} \int_0^\ell u \cdot d_*(u) du - 1,$$

which implies:

$$\int_0^\ell u \cdot d_*(u) du = \frac{\ell}{2}(S_\ell + 1).$$

Substituting into the expression for  $S_L$ :

$$\begin{aligned} S_L &= \frac{2}{L} \left( \frac{\ell}{2}(S_\ell + 1) + (L - \ell) \right) - 1 \\ &= \frac{1}{L} (\ell(S_\ell + 1) + 2(L - \ell)) - 1 \\ &= \frac{1}{L} (\ell S_\ell - \ell + 2L) - 1 \\ &= \frac{\ell(S_\ell - 1) + 2L}{L} - 1 \\ &= \frac{\ell(S_\ell - 1)}{L} + 2 - 1 \\ &= 1 + \frac{\ell}{L}(S_\ell - 1) \end{aligned}$$

Therefore, the forward transformation is:

$$S_L = 1 + \left( \frac{\ell}{L} \right) (S_\ell - 1)$$

This formula expresses, given arbitrary domains with measures  $L$  and  $\ell$  (where  $L > \ell$ ), and the sharpness score  $S_\ell(d_*)$  of a probability density function  $d$  defined over a domain of measure  $\ell$ , the sharpness score  $S_L$  of  $d$  over  $L$ , where  $d(y) = 0$  for all  $y$  in the extended region.

#### S2.2.0.2 Inverse Transformation (from $L$ to $\ell$ ):

Assume that  $d: B \rightarrow \mathbb{R}_{\geq 0}$  is a probability density function such that  $d(y) = 0$  for all  $y \in B \setminus A$ , where  $A \subset B \subset \mathbb{R}^n$  are measurable sets with  $\lambda(A) = \ell$ ,  $\lambda(B) = L$ , and  $L > \ell$ .

We recover  $S_\ell$  from the sharpness score  $S_L$  of the extended density  $d$  over  $B$  by rearranging the forward transformation formula:

$$\begin{aligned} S_L &= 1 + \left(\frac{\ell}{L}\right) (S_\ell - 1) \\ S_L - 1 &= \left(\frac{\ell}{L}\right) (S_\ell - 1) \\ S_\ell - 1 &= \left(\frac{L}{\ell}\right) (S_L - 1) \end{aligned}$$

Therefore, the inverse transformation is:

$$S_\ell = 1 + \left(\frac{L}{\ell}\right) (S_L - 1)$$

The inverse operation reverses the extension added by the zero-density regions and rescales the result from normalization over measure  $L$  to normalization over measure  $\ell$ . Thus, this formula expresses, given arbitrary domains with measure  $L$  and  $\ell$  (where  $L > \ell$ ) and the sharpness score  $S_L(d_*)$  of a probability density function  $d$  defined over  $L$ , the sharpness score  $S_\ell(d_*)$  of the restriction of  $d$  to the subdomain of measure  $\ell$ , assuming that  $d(y) = 0$  for all  $y$  in the extended region. This formula enables truncating regions of the larger domain where the density is zero and rescaling the sharpness score to the subregion of interest.

## S3 Formulas for Analysis in the Rearranged Space

The mass-length functional representation of the sharpness measure  $S(d_*)$  provides a structured space in which aspects of the original probability distribution  $d$  can be represented alongside the global sharpness measure. This section outlines how to recover points or regions of interest from the original distribution, assess local contributions to sharpness score, and evaluate diagnostic quantities such as relative rank and mass above a density threshold in the rearranged space.

### S3.1 Mapping from Original Domain to Rearranged Space

Let  $y_p \in \Omega$  be a point (e.g., represented by a narrow interval) in the original outcome space, and let  $d(y_p)$  be its density under  $d$ . To locate the approximate rearranged position  $t_p \in [0, |\Omega|]$  of  $y_p$ , we match  $d(y_p)$  to the value of  $d_*(t)$  over a uniform discretization  $\{t_i\}_{i=1}^N$ :

$$t_p = t_j \quad \text{where} \quad j = \arg \min_i |d_*(t_i) - d(y_p)|.$$

This mapping identifies a corresponding point in the rearranged domain whose density is closest to that of  $y_p$ . If multiple points in the original domain share the same density, their mapping to  $t$  is non-unique. However, in this case, the rearranged function  $d_*(t)$  is constant over a subinterval  $I \subset [0, |\Omega|]$ , that is,  $d_*(t) = \tau$  for all  $t \in I$ . Over such an interval, the mass-length functional representation exhibits linear structure: the remaining mass function  $m(t) = \int_t^{|\Omega|} d_*(s) ds$  decreases linearly when  $\tau > 0$ , and remains constant when  $\tau = 0$ ; likewise, the term  $d_*(t) \cdot L(t)$  decreases linearly when  $\tau > 0$  and remains constant when  $\tau = 0$ . As a result, the sharpness integrand  $m(t) - d_*(t) \cdot L(t)$  forms an affine segment, whose slope is zero if and only if  $\tau = 0$ . This geometric behavior encodes the rank and measure of the equal-density region in the rearranged space, even though the original spatial locations of the values are not preserved. Figure S1 illustrates the behavior of the mass-length functional over several representative probability density functions.

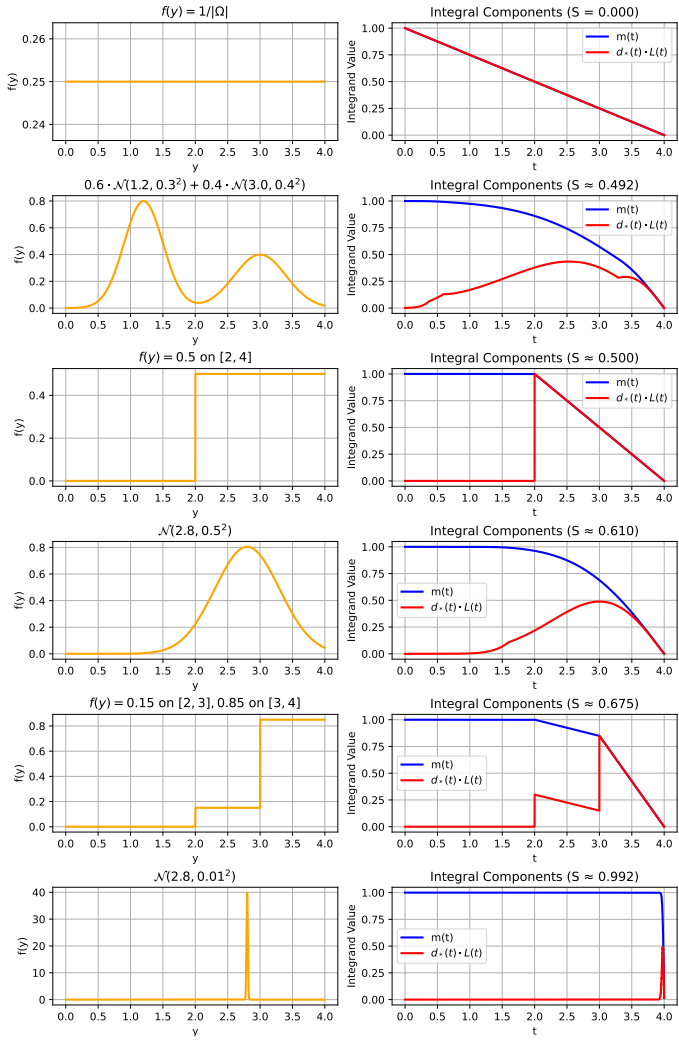


Figure S1: Plots for some of the probability distribution functions in Table 2 of the article and the integral components of  $S(d_*)$ .

### S3.2 Recovering Key Points

Key reference points in the original probability distribution  $d$ —such as the mean, median, or an observed value—can be approximately located in the rearranged domain by matching their density values to the sorted profile  $d_*(t)$ . Let  $d_*(t)$  be evaluated on a uniform grid  $\{t_1, \dots, t_N\}$  over  $[0, |\Omega|]$ , with spacing  $\Delta t = |\Omega|/N$ .

**S3.2.0.1 Mode.** Let  $y_{\text{mode}} \in \Omega$  be a mode of the original distribution, such that

$$d(y_{\text{mode}}) = \max_{y \in \Omega} d(y).$$

To find its position in rearranged space, identify the index  $j$  such that:

$$t_{\text{mode}} = t_j \quad \text{where} \quad j = \arg \min_i |d_*(t_i) - d(y_{\text{mode}})|.$$

**S3.2.0.2 Median.** Let  $y_{\text{med}} \in \Omega$  be defined as:

$$y_{\text{med}} = \inf \left\{ y \in \Omega \mid \int_a^y d(y') dy' \geq \frac{1}{2} \right\},$$

where  $a = \inf \Omega$  is the lower bound of the domain. Then, identify its location in the rearranged space by:

$$t_{\text{med}} = t_j \quad \text{where} \quad j = \arg \min_i |d_*(t_i) - d(y_{\text{med}})|.$$

**S3.2.0.3 Mean.** The mean of the distribution is given by

$$y_{\text{mean}} = \int_{\Omega} y d(y) dy.$$

Let  $d(y_{\text{mean}})$  denote its density under  $d$ . The corresponding position in the rearranged space can be identified by:

$$t_{\text{mean}} = t_j \quad \text{where} \quad j = \arg \min_i |d_*(t_i) - d(y_{\text{mean}})|.$$

**S3.2.0.4 Specific point (e.g., observed value).** For a specific outcome  $y_p \in \Omega$ , define:

$$t_p = t_j \quad \text{where} \quad j = \arg \min_i |d_*(t_i) - d(y_p)|.$$

These mappings allow us to recover salient points from the original distribution  $d$ . When a point  $y_p \in \Omega$  lies in a region of constant density—that is, when  $d(y_p) = \tau$  and there exists a maximal interval  $I_y = [a, b] \subset \Omega$  such that  $d(y) = \tau$  for all  $y \in I_y$ —the non-decreasing

rearrangement  $d_*(t)$  will likewise be constant over an interval  $I_t = [t_a, t_b] \subset [0, |\Omega|]$  of the same measure. Thus, an alternative approach is not to map  $y_p$  to a single point, but instead to identify the entire constant region in the rearranged space. In practice, this is done by scanning  $d_*(t)$  for all indices  $t_i$  such that

$$|d_*(t_i) - \tau| \leq \varepsilon,$$

for a small numerical tolerance  $\varepsilon$ . The first and last such indices define the endpoints  $t_a$  and  $t_b$  of the plateau region in rearranged space:

$$I_t = [t_a, t_b].$$

### S3.3 Local Contribution to Sharpness

To compute the contribution of a specific region of the rearranged space to the total sharpness score, we use the mass-length decomposition. Let  $[t_a, t_b] \subseteq [0, |\Omega|]$  be a subinterval of the rearranged domain. The normalized contribution of this region to the overall sharpness score is given by:

$$\Delta([t_a, t_b]) = \frac{1}{|\Omega|} \int_{t_a}^{t_b} (m(t) - d_*(t)L(t)) dt,$$

where  $m(t) = \int_t^{|\Omega|} d_*(s) ds$  is the remaining mass, and  $L(t) = |\Omega| - t$  is the remaining length.

The contribution of a narrow sliver (e.g., one bin in a discretization) is given by:

$$\Delta(t_i) \approx \frac{1}{|\Omega|} (m(t_i) - d_*(t_i)L(t_i)) \cdot \Delta t,$$

where  $t_i$  is the location of the sliver and  $\Delta t$  is its width.

In addition to computing contributions in the rearranged domain, it is also useful to evaluate the contribution of regions defined in the original outcome space. Let  $A \subseteq \Omega$  be a measurable region, for example an interval or a rectangular region in multiple dimensions.

The corresponding set of densities  $\{d(y) : y \in A\}$  can be mapped onto the rearranged space using the approach described above (S3.2.0.4) (equal densities contribute equally to the sharpness score, so any equal densities can be mapped to the same index). Denote by  $T(A) \subseteq [0, |\Omega|]$  the set of rearranged indices associated with region  $A$ . Then the local contribution of  $A$  to the sharpness score is computed as

$$\Delta(A) \approx \frac{1}{|\Omega|} \sum_{t_i \in T(A)} (m(t_i) - d_*(t_i)L(t_i)) \Delta t,$$

where  $\Delta t = |\Omega|/N$  is the grid resolution.

### S3.4 Mapping Support for a Region in the Rearranged Space

Suppose we are given a measurable subregion  $A \subseteq \Omega$  and we wish to examine its support in the rearranged space. To assess whether any part of the region is supported, we check whether  $d(y) > 0$  for some  $y \in A$ . In the rearranged representation, the corresponding positive densities from  $A$  can then be located using the approach defined in Section S3.2. The indices  $t_i$  associated with positive densities identify the part of the rearranged domain linked to  $A$ . Visualizing these positions in the rearranged space allows simultaneously displaying multiple properties of the chosen region, including relative rank and mass allocated to higher density regions (see below).

### S3.5 Mass Above a Density Threshold

Given a point  $y_p \in \Omega$ , let  $t_p \in [0, |\Omega|]$  be its corresponding location in the rearranged space, identified via

$$t_p = t_j \quad \text{where} \quad j = \arg \min_i |d_*(t_i) - d(y_p)|.$$

Define the density level at this location as  $\tau = d_*(t_p)$ . Then, the mass allocated to all higher-density outcomes is:

$$M_*(\tau) = \int_{\{t \in [0, |\Omega|] : d_*(t) > \tau\}} d_*(t) dt.$$

This is implemented by locating the first point in the rearranged space with density strictly greater than  $\tau$  and computing the cumulative remaining mass  $m(t)$  from that point onward.

### S3.6 Relative Likelihood and Rank

Let  $y_p \in \Omega$  be a point in the original space, with density  $d(y_p)$ . The relative likelihood of  $y_p$  is defined as its density relative to the maximum density of the distribution:

$$\text{RL}(y_p) = \frac{d(y_p)}{\max_{y \in \Omega} d(y)}.$$

Since each density value corresponds to a location in the rearranged space, the relative likelihood can also be calculated in the rearranged space by mapping  $d(y_p)$  to its corresponding density in  $d_*(t)$  and examining it in relation to a mode of the distribution.

The relative rank of  $y_p$  can be represented in the rearranged space by examining the proportion of rearranged domain points with lower density than  $d(y_p)$ :

$$R(y_p) = \frac{1}{N} \cdot |\{i \mid d_*(t_i) < d(y_p)\}|,$$

where  $\{t_i\}_{i=1}^N$  denotes the discretization of the rearranged space.

### S3.7 Summary Table

Quantity	Recovery Formula
Mode	$t_{\text{mode}} = t_j, j = \arg \min_i  d_*(t_i) - d(y_{\text{mode}}) $
Median	$t_{\text{med}} = t_j, j = \arg \min_i  d_*(t_i) - d(y_{\text{med}}) $
Mean	$t_{\text{mean}} = t_j, j = \arg \min_i  d_*(t_i) - d(y_{\text{mean}}) $
Specific point	$t_p = t_j, j = \arg \min_i  d_*(t_i) - d(y_p) $
Mass above	$\tau = d_*(t_p), M_*(\tau) = \int_{\{t \in [0,  \Omega ] : d_*(t) > \tau\}} d_*(t) dt$
Local contribution (rearranged)	$\Delta([t_a, t_b]) = \frac{1}{ \Omega } \int_{t_a}^{t_b} (m(t) - d_*(t)L(t)) dt$
Local contribution (original)	$\Delta(A) \approx \frac{1}{ \Omega } \sum_{t_i \in T(A)} (m(t_i) - d_*(t_i)L(t_i)) \Delta t$
Relative likelihood	$RL(y_p) \approx \frac{d_*(t_p)}{d_*(t_{\text{mode}})}$
Relative rank	$R(y_p) \approx \frac{1}{N} \cdot  \{i \mid d_*(t_i) < d(y_p)\} $

Table S1: Key quantities approximated in the rearranged space  $d_*(t)$ , derived from a distribution  $d$  on  $\Omega$ .

## S4 Analysis of Sharpness, Entropy, and Variance

This section investigates the relationships between sharpness, entropy, and variance, three complementary measures that can be used to characterize the shape and spread of probability distributions. To demonstrate the complementary diagnostic information that these measures provide, we focus on level sets of these measures: collections of distributions that share approximately equal values of sharpness, entropy, or variance, respectively. For visualization, we restrict attention to discrete distributions. The accompanying material to this article includes Python scripts for reproducing the visualizations in this section.

## S4.1 Level Sets on the 2-Simplex

We begin by analyzing distributions on the 2-simplex, which represents the space of all probability vectors  $(p_1, p_2, p_3) \in \mathbb{R}^3$  satisfying  $p_i \geq 0$  and  $\sum_{i=1}^3 p_i = 1$ . Each point on the simplex corresponds to a discrete distribution over three outcomes. Within this space, the sharpness, entropy, and variance functionals partition the simplex into level sets—subsets of distributions that yield approximately the same value under the respective measure.

Figure S2 displays the sharpness level set corresponding to  $S(P) \approx 0.5$ . To contextualize the geometry of this level set, we partition the 2-simplex into six regions, each corresponding to a distinct permutation of the probabilities  $(p_1, p_2, p_3)$ . These regions are determined by the relative ordering of the three components and are delineated by boundary lines where two probabilities are equal (e.g.,  $p_1 = p_2$ ). The vertices correspond to distributions where the respective outcome is given probability 1.0. The uniform distribution  $(1/3, 1/3, 1/3)$  lies at the center, invariant under permutation.

**Sharpness Set  $\approx 0.5$  and Permutation Regions ( $n = 3$ )**

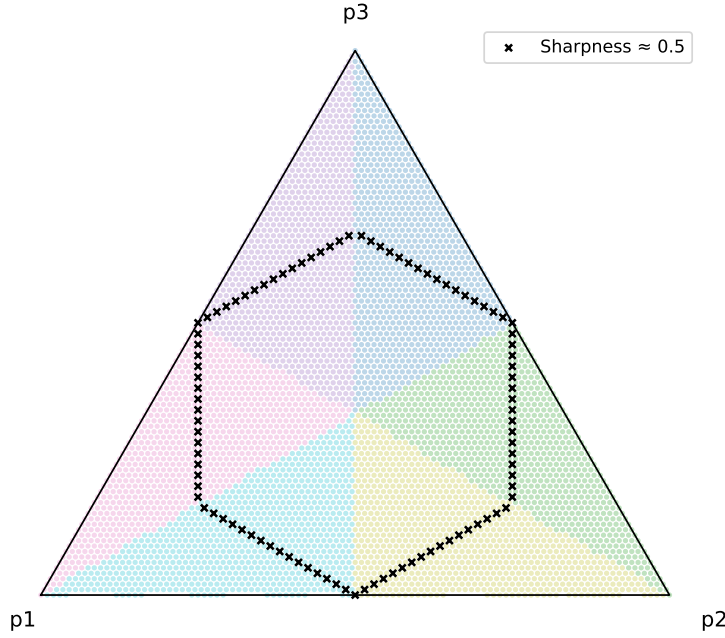


Figure S2: The set of distributions where sharpness is approximately 0.5 on the 2-simplex.

The six regions are described as follows, moving clockwise from the top vertex:

1. **Top right (blue):**  $p_1 < p_2 < p_3$
2. **Right middle (green):**  $p_1 < p_3 < p_2$
3. **Bottom right (yellow):**  $p_3 < p_1 < p_2$
4. **Bottom left (light blue):**  $p_3 < p_2 < p_1$
5. **Left middle (pink):**  $p_2 < p_3 < p_1$
6. **Top left (violet):**  $p_2 < p_1 < p_3$

To compare the behavior of the different measures, Figure S3 displays level sets of entropy, variance, and sharpness on the 2-simplex. Each measure partitions the space in a distinctive way, reflecting its particular sensitivity to aspects of distributional structure (uncertainty, spatial dispersion, and concentration).

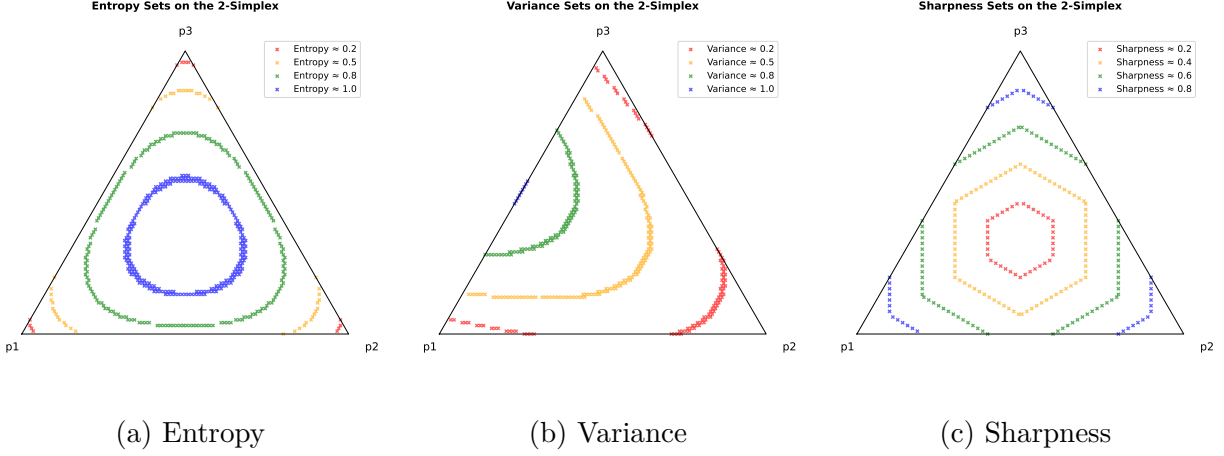


Figure S3: Level sets of entropy, variance, and sharpness on the 2-simplex.

Entropy reflects the total uncertainty of the distribution, and it is maximized when each outcome is given equal probability and decreasing when uncertainty over the outcomes is reduced. Sharpness tracks the concentration of mass within the distribution, reflecting the displacement of mass from low probability regions to high probability regions. Both entropy and sharpness are invariant under permutation. Variance is sensitive to the spatial position of outcomes, so naturally it is minimized when mass is centered and maximized when mass is split between outcomes at opposite ends of the outcome index.

## S4.2 Level Sets on the 3-Simplex

The same behavior can be observed when examining the space of discrete probability distributions over four outcomes. Distributions over four outcomes can be analyzed on the 3-simplex, which is defined by:

$$\Delta^3 = \left\{ (p_1, p_2, p_3, p_4) \in \mathbb{R}^4 \mid p_i \geq 0, \sum_{i=1}^4 p_i = 1 \right\}.$$

The 3-simplex is visualized as a regular tetrahedron in  $\mathbb{R}^3$ , where each vertex again corresponds to a degenerate distribution concentrated entirely on one outcome. Here, the level sets of the measures trace out a thin surface embedded within the simplex, displaying the

characteristic geometric imprint of the corresponding measure.

Figure S4 shows representative level sets of sharpness and entropy. Both measures show their unique imprint, reflecting related but distinctive aspects of distributional structure. Although the measures generally vary inversely, where sharpness increases as entropy decreases, the measures hook into distinct properties: entropy quantifies total uncertainty, while sharpness captures concentration over the domain.

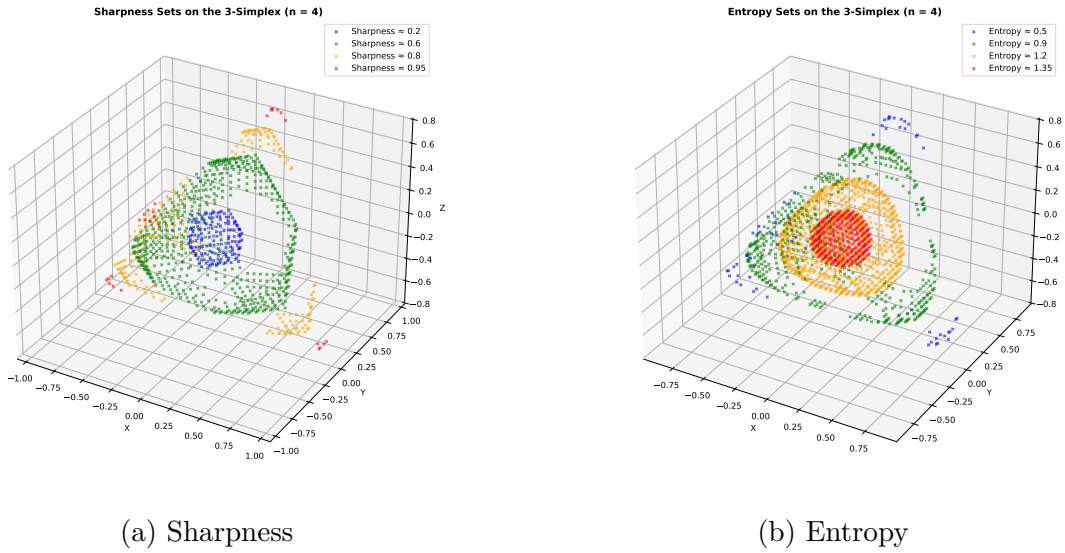


Figure S4: Level sets of sharpness and entropy on the 3-simplex.

Figure S5 shows representative level sets of variance. Very different distributions can lie on the same level set if they spread mass across outcomes in such a way that overall difference from the mean is preserved. The levels sets are stretched along directions where mass is distributed more evenly across outcomes, and compressed along directions where the distribution becomes increasingly dominated by an outlier value.

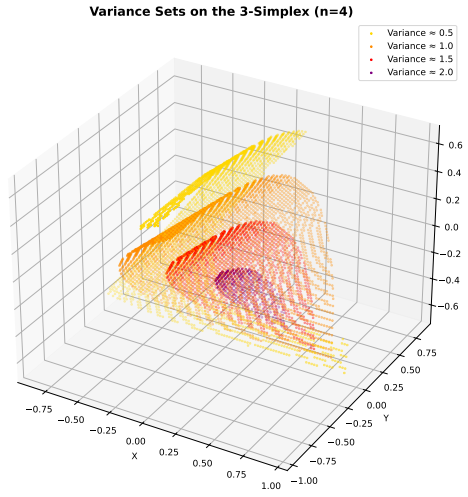


Figure S5: Variance level sets on the 3-simplex.

### S4.3 Variation Over Level Sets

Given the distinctive behavior of each measure, they jointly provide a more detailed characterization of distributional shape. Sharpness and variance, in particular, exhibit a reciprocal relationship: variance measures spatial dispersion as sharpness measures concentration. Considered together, they distinguish between more or less sharp and more or less spatially spread out distributions within each other's level sets, revealing differences in distributional shape that either measure alone would miss. Sharpness and entropy, by contrast, have a more complex relationship: for a given sharpness set, entropy is minimized by distributions that exhibit more regular structure; namely, distributions that spread mass equally among a subset of the outcomes or, particularly with greater sharpness scores, single-peaked distributions. For a given entropy set, sharpness is maximized by more concentrated distributions, achieved through peakedness, or at lower entropy, by more confident suppression of low probability outcomes.

We begin by exploring the relationship between entropy and sharpness. Figure S6 illustrates how the two measures vary with respect to one another on the 2-simplex.

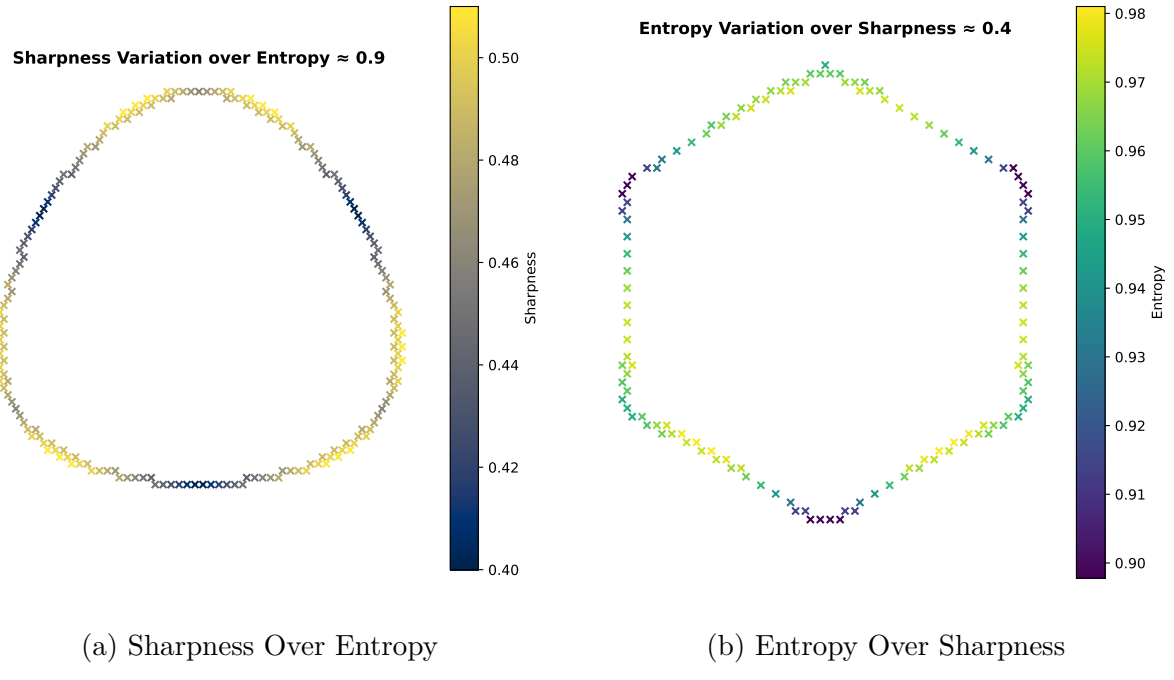


Figure S6: Level sets of entropy and sharpness for  $n=3$ , with sharpness and entropy variation overlaid.

When sharpness is overlaid on entropy, its minimum values occur for the flattest distributions consistent with the entropy constraint. For example, for entropy level set  $H(P) \approx 0.9$ , distributions with minimal sharpness include distributions such as  $\{0.07, 0.46, 0.47\}$ . Within the same entropy level set, sharpness increases as the distribution becomes more concentrated, with one outcome absorbing a disproportionate share of the mass (e.g., here,  $\{0.11, 0.27, 0.62\}$ ). Similarly, when entropy is overlaid on sharpness level sets, entropy is lowest when the distribution balances mass between a subset of the outcomes—for sharpness level set  $S(P) \approx 0.4$ , which corresponds roughly to the previous entropy level set, again when two of the three probabilities are nearly equal (e.g.,  $\{0.48, 0.45, 0.07\}$ ). Within the same sharpness level set, entropy is maximized when the mass is distributed unevenly across the outcomes while still maintaining the sharpness constraint (e.g.,  $\{0.55, 0.29, 0.16\}$ ).

Figure S7 illustrates this behavior when  $n=4$ . Within the entropy level set, sharpness is

minimized by the most equal distributions—for example,  $\{0, 0.22, 0.38, 0.4\}$ , with  $S(P) \approx 0.45$  for entropy  $\approx 1.05$ —and maximized by concentration within the distribution—for example,  $\{0.6, 0.24, 0.04, 0.12\}$ , with  $S(P) = 0.6$  for entropy  $\approx 1.05$ . For a moderately high sharpness score of 0.7, entropy is minimized by balancing mass between a subset of outcomes—e.g.,  $\{0, 0, 0.45, 0.55\}$ , with  $H(P) \approx 0.69$ —and maximized by uneven distributions—e.g.,  $\{0.68, 0.07, 0.03, 0.22\}$ , with  $H(P) \approx 0.89$ .

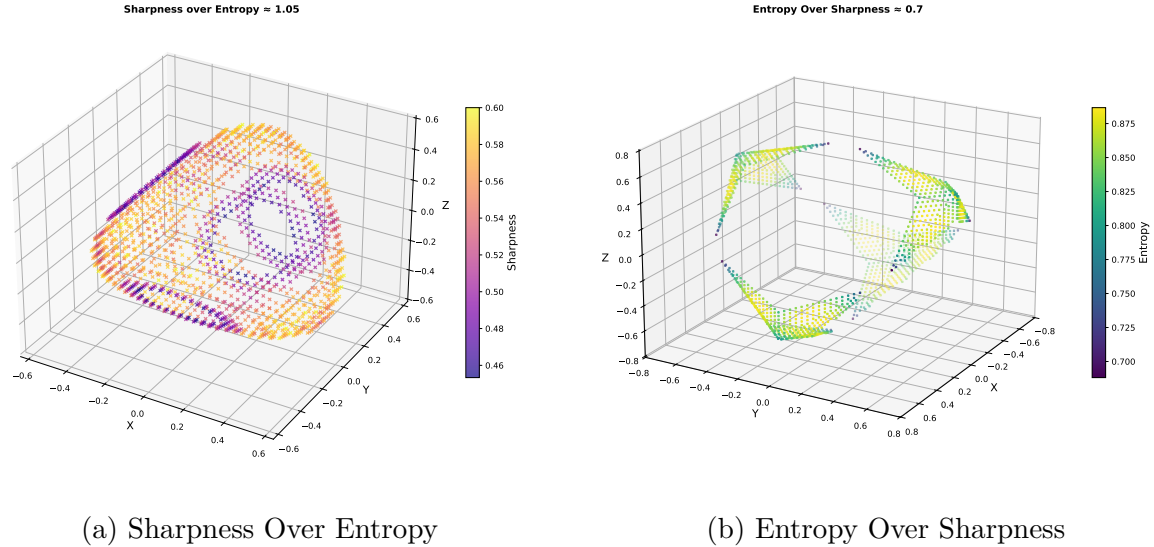
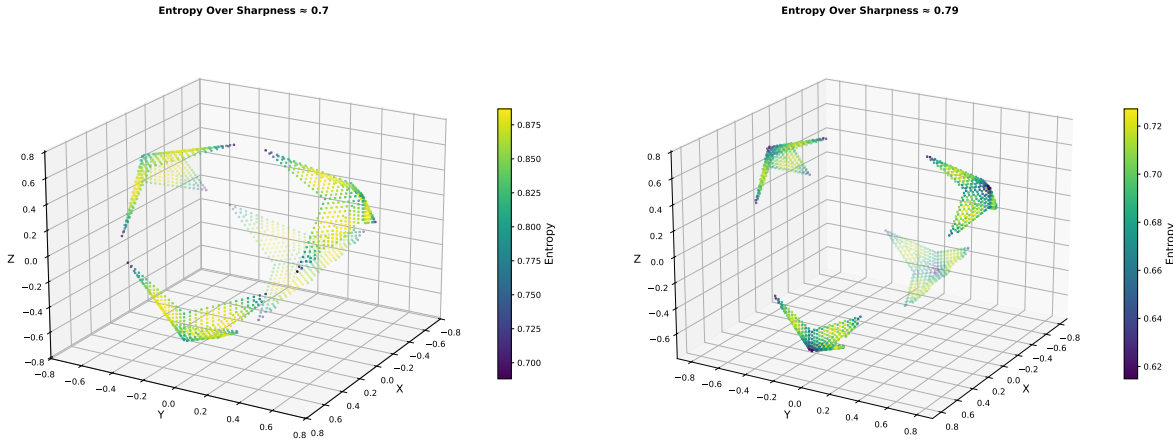


Figure S7: Level sets of sharpness and entropy for  $n=4$ , with entropy and sharpness overlaid.

This reciprocal behavior arises because within sharpness level sets, entropy captures disorganization within the distribution: more disorganized distributions (i.e., those with more unevenly distributed probability mass) achieve highest entropy, while the most organized distributions have the lowest entropy. However, notably, organization within a distribution can be achieved in either of two ways: either by balancing probability mass between a subset of the outcomes, or by concentrating on a peak value. When sharpness scores increase, the latter type begins to dominate, and low entropy signifies a single-peaked rather than a subset-focused distribution. This is illustrated in Figure S8.



(a) Entropy Over Sharpness  $\approx 0.70$

(b) Entropy Over Sharpness  $\approx 0.79$

Figure S8: Sharpness levels sets with entropy overlaid for  $n=4$ .

For  $S(P) \approx 0.70$ , low entropy distributions are still dominated by distributions that spread mass more evenly between a subset of the outcomes (here, between the two highest probability outcomes, as noted above). However, when mass can no longer be distributed between multiple outcomes to maintain the high sharpness constraint, the lowest entropy distributions shift to single-peaked distributions within the level set. For  $n=4$ , this occurs around  $S(P) \approx 0.79$ , where lowest entropy distributions now include single-peaked distributions such as  $\{0.05, 0.05, 0.84, 0.06\}$  with  $H(P) \approx 0.61$ , and highest entropy ones include more disorganized distributions such as  $\{0.19, 0.75, 0.05, 0.01\}$ , with  $H(P) \approx 0.73$ .

Sharpness behaves in reciprocal fashion. Similarly to minimizing entropy within a sharpness level set, there are two alternative ways to increase sharpness within an entropy level set: either by concentrating mass on a peak value (or, for lower sharpness scores, a set of peak values), or by suppressing low probability outcomes. The former type is prevalent for higher entropy distributions, while for low entropy level sets, sharpness slightly favors more confident suppression over peakedness. For  $n=4$ , sharpness is highest for peaked distributions up to  $H(P) \approx 0.57$ , where maximum sharpness is achieved by distributions

such as  $\{0.83, 0.13, 0.03, 0.01\}$  with  $S(P) \approx 0.853$  and minimum by distributions such as  $\{0, 0, 0.26, 0.74\}$  with  $S(P) \approx 0.827$ . At  $H(P) \approx 0.56$ , a similar shift occurs mirroring that of entropy, where the lowest sharpness scores within the entropy level set are given by distributions that retain more outcomes but peak on the highest value (e.g.,  $\{0.04, 0.05, 0.05, 0.86\}$  with  $S(P) = 0.82$ ) while highest sharpness scores are achieved by distributions that more strongly suppress low probability outcomes (e.g.,  $\{0.01, 0.01, 0.17, 0.81\}$  with  $S(P) \approx 0.85$ ).

For growing values of  $n$ , similar behaviors are maintained: low entropy signifies organization—achieved via evenly balanced subsets or concentration at a single value—and sharpness reflects concentration—achieved via peakedness at the top of the rearranged space or suppression of low probability outcomes. However, given the growing number of permutations, both measures can reward either strategy for a wider range of respective sharpness or entropy level sets. For example, in a sample of 5 000 000 distributions over  $n=10$ , and given a sharpness level set  $S(P) \approx 0.4$ , lowest entropy values were achieved by more even distributions (e.g., distributions with 7 outcomes sharing roughly equal probability). By contrast, for sharpness level set  $S(P) \approx 0.6$ , distributions where one outcome has a disproportionate share of mass achieved the lowest entropy. In either case, disorganized distributions, where the outcomes have more varied probabilities, achieved the highest entropy. For entropy level set  $H(P) \approx 1.0$ , sharpness slightly favored tail suppression over peakedness, while for  $H(P) \approx 2.0$ , it favored peakedness (which, for a sharpness score of 0.49 for  $n=10$ , was achieved by concentrating mass over a subset of two outcomes). In either case, sharpness strongly favored concentrated distributions over flat distributions.

In addition to entropy and sharpness, variance provides additional diagnostic value by quantifying the spatial dispersion of the probability mass. Variance can remain constant across distributions with vastly different sharpness scores, and vice versa. This complementary behavior is illustrated in Figure S9 on the 2-simplex ( $n=3$ ).

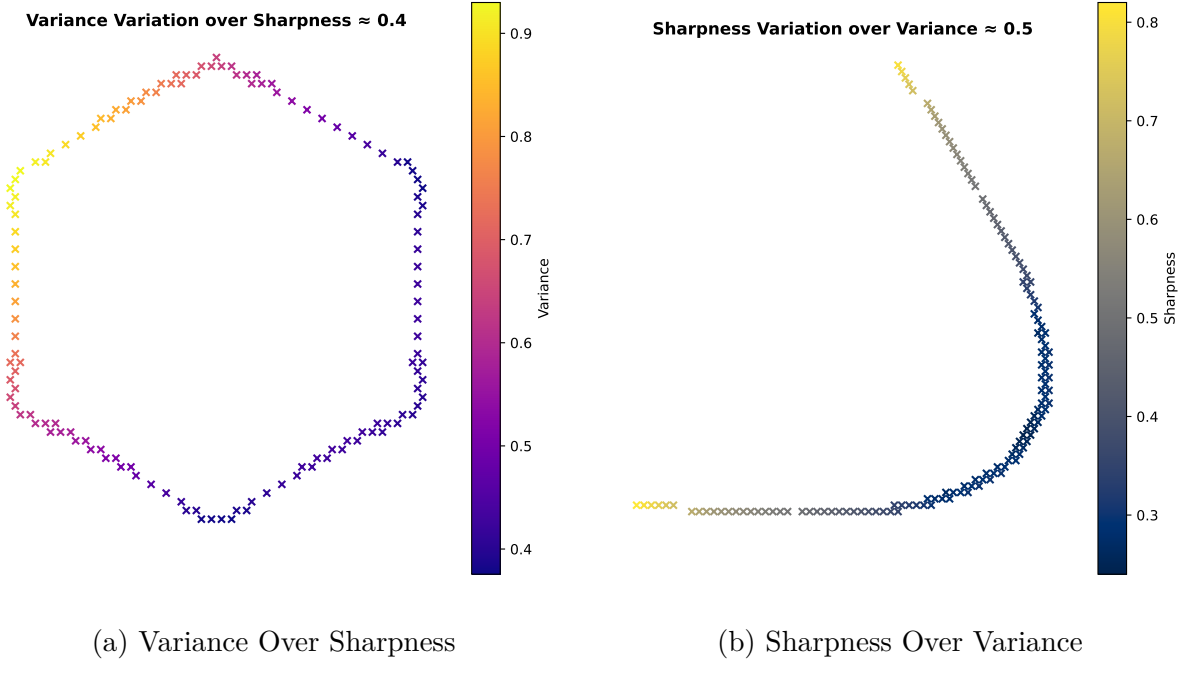


Figure S9: Level sets of sharpness and variance for  $n=3$ , with variance and sharpness overlaid.

For  $n=3$  and sharpness level set  $S(P) \approx 0.4$ , distributions such as  $\{0.47, 0.07, 0.46\}$  maximize variance, while variance is minimized by concentrating mass over adjacent positions (e.g.,  $\{0.45, 0.48, 0.07\}$ ). Conversely, sharpness score is lowest when the distribution is flat and highest when it is highly concentrated. For example, for variance level set  $Var(P) \approx 0.5$ , distributions such as  $\{0.25, 0.49, 0.26\}$  yield the lowest sharpness scores (e.g., here,  $S(P) = 0.24$ ), while distributions where one value dominates, such as  $\{0.84, 0.02, 0.14\}$ , yield a considerably higher score—here,  $S(P) = 0.82$ .

Figure S10 illustrates variance over sharpness when  $n=4$ . The highest variance region corresponds to the distributions where mass is concentrated at the opposite ends of the domain. In this case, where  $S(P) \approx 0.70$ , variance is maximized by distributions such as  $\{0.44, 0, 0, 0.56\}$  and minimized by distributions such as  $\{0, 0.44, 0.56, 0\}$ .

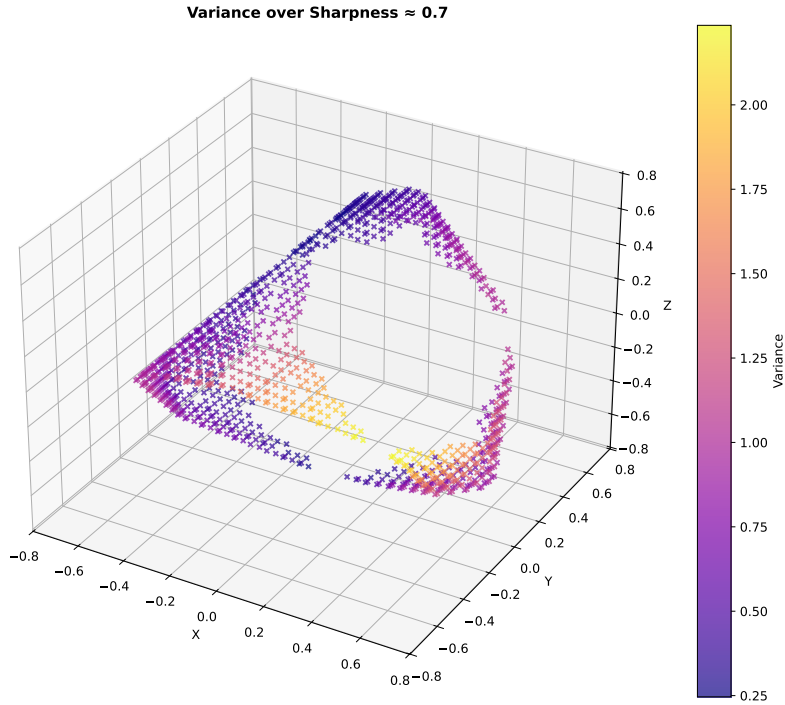


Figure S10: Sharpness level set  $S(P) \approx 0.7$  on the 3-simplex, with variance overlaid.

Finally, Figure S11 illustrates sharpness over variance level set  $Var(P) \approx 1.0$ . In this case, the range between the lowest and highest sharpness scores is extreme: a low of  $S(P) \approx 0.17$  is achieved by  $\{0.19, 0.32, 0.3, 0.19\}$ , while a high of  $S(P) \approx 0.89$  is achieved by  $\{0.12, 0.02, 0, 0.86\}$ . Given the behavior of each measure, the relationship between sharpness and variance is naturally maintained for higher values of  $n$ , where sharpness is highest for the most concentrated distributions while variance is maximized by packing mass at opposite ends of the domain.

**Sharpness over Variance  $\approx 1.0$**

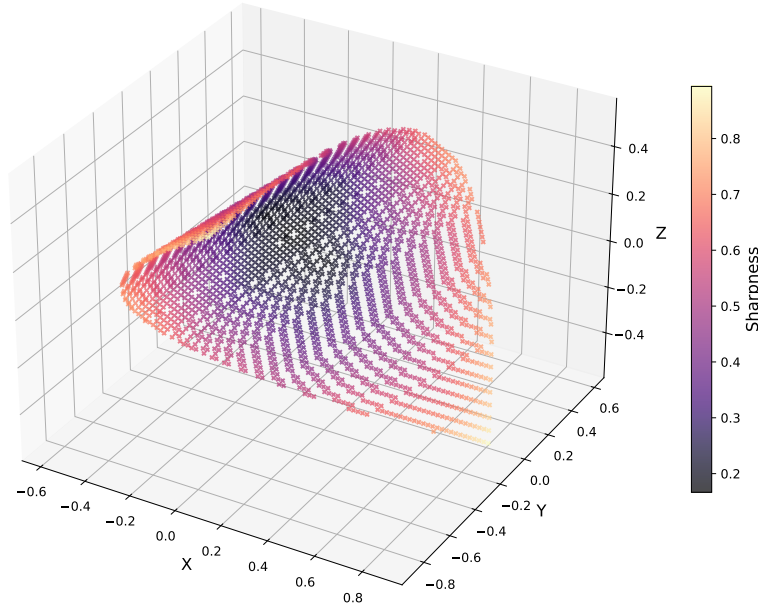


Figure S11: Variance level set  $Var(P) \approx 1.0$  on the 3-simplex, with sharpness overlaid.

For continuous cases, visualization becomes more difficult; however, the basic relationships between the three measures are preserved. For example, in a sample of 100 000 unimodal and bimodal Gaussian distributions defined over domain of measure 6, and given sharpness level set  $S(d_*) \approx 0.6$ , variance was minimized by a centered unimodal distribution and maximized by a bimodal distribution where the peaks occur at the ends of the domain. For bimodal distributions and a given sharpness set, entropy was minimized by distributions where the peaks are roughly equal, and maximized by unequal peaks. Conversely, sharpness scores increase when probability mass becomes more unequally concentrated within the distribution.